2-Aminothiazole as a Novel Kinase Inhibitor Template. Structure−Activity Relationship Studies toward the Discovery of *N*-(2-Chloro-6-methylphenyl)-2-[[6-[4-(2-hydroxyethyl)-1-piperazinyl)]-2-methyl-4-pyrimidinyl]amino)]-1,3-thiazole-5-carboxamide (Dasatinib, BMS-354825) as a Potent *pan*-Src Kinase Inhibitor

Jagabandhu Das,* Ping Chen,* Derek Norris, Ramesh Padmanabha,† James Lin, Robert V. Moquin, Zhongqi Shen, Lynda S. Cook,† Arthur M. Doweyko, Sidney Pitt, Suhong Pang, Ding Ren Shen, Qiong Fang, Henry F. de Fex, Kim W. McIntyre, David J. Shuster, Kathleen M. Gillooly, Kamelia Behnia, Gary L. Schieven, John Wityak, and Joel C. Barrish

Bristol-Myers Squibb Pharmaceutical Research Institute, Post Office Box 4000, Princeton, New Jersey 08543-4000, and Bristol-Myers Squibb Pharmaceutical Research Institute, Wallingford, Connecticut

Received June 15, 2006

2-Aminothiazole (**1**) was discovered as a novel Src family kinase inhibitor template through screening of our internal compound collection. Optimization through successive structure−activity relationship iterations identified analogs **2** (Dasatinib, BMS-354825) and **12m** as *pan*-Src inhibitors with nanomolar to subnanomolar potencies in biochemical and cellular assays. Molecular modeling was used to construct a putative binding model for Lck inhibition by this class of compounds. The framework of key hydrogen-bond interactions proposed by this model was in agreement with the subsequent, published crystal structure of **2** bound to structurally similar Abl kinase. The oral efficacy of this class of inhibitors was demonstrated with **12m** in inhibiting the proinflammatory cytokine IL-2 ex vivo in mice ($ED_{50} \sim 5$ mg/kg) and in reducing TNF levels in an acute murine model of inflammation (90% inhibition in LPS-induced TNFα production when dosed orally at 60 mg/kg, 2 h prior to LPS administration). The oral efficacy of **12m** was further demonstrated in a chronic model of adjuvant arthritis in rats with established disease when administered orally at 0.3 and 3 mg/kg twice daily. Dasatinib (**2**) is currently in clinical trials for the treatment of chronic myelogenous leukemia.

Introduction

Mammalian immunity relies on activation of T cells upon antigen presentation. Immune responses in T cells are initiated by interaction of the T-cell antigen receptor (TCR[a]) with an antigen presented in the context of a glycoprotein encoded by the major histocompatability complex (MHC). Upon its engagement T-cell activation is amplified by sequential activation of three distinct classes of nonreceptor tyrosine kinases, namely, the Src family kinases ($p56^{Lck}$ and Fyn), the Syk family kinases (Syk and ZAP-70), and the Tec family kinases (Itk, Txk, and Tec). A cascade of downstream signaling pathways ultimately leads to T-cell proliferation and/or differentiation and production of proinflammatory cytokines such as interleukin-2 (IL-2).

$p56^{Lck}$ (Lck) is a member of the Src family of nonreceptor tyrosine kinases that share a high degree of homology, particularly at the ATP binding pocket. Lck, expressed predominantly in T cells and NK cells is absolutely required for T-cell development,[1] activation,[2] and initiation of the T-cell antigen receptor (TCR)-mediated signal transduction pathway. Studies have shown that the catalytic activity of Lck is regulated by phosphorylation of Tyr394 in the catalytic domain and Tyr505 at the C-terminus. Upon autophosphorylation, activated Lck phosphorylates tyrosine residues in the immunoreceptor tyrosine activation motif (ITAM) sequences of the invariant chains (including the ζ chain) within the TCR. Once phosphorylated, the ζ chain provides docking sites for ZAP-70 binding via its SH2 domains.[2c] Phosphorylation of ZAP-70 by Lck and the combined action of ZAP-70, Lck, and the related Src family kinase Fyn drives downstream signaling events and leads ultimately to calcium flux, T-cell activation, and proliferation (Figure 1). Genetics experiments using $Lck^{-/-}$ mice have validated Lck as a potential immunosuppressive molecular target.[1a] These mice display a SCID-like syndrome and are unable to reject skin grafts despite the presence of peripheral T cells.[3] In addition, overexpression of a dominant negative form of Lck leads to early arrest of thymocyte development prior to expression of CD4, CD8, and the TCR.[1b] Based on these data, an Lck inhibitor should inhibit T-cell activation and have potential utility in the treatment of acute and chronic T-cell mediated autoimmune and inflammatory disorders, including solid organ transplant graft rejection, multiple sclerosis, rheumatoid arthritis (RA), psoriasis, and delayed type hypersensitivity reactions.[4] In addition, dysregulation of Lck expression or its kinase activity has also been implicated in human T-cell leukemia,[5] lymphocytic B cell leukemia,[6] human colon carcinoma,[7] and small cell lung cancer.[8]

The c-Src proto-oncogene also plays a central role in the development and progression of several human cancers, including colon, breast, pancreatic, lung, and brain cancers.[9,10] Src kinase modulates signal transduction through multiple oncogenic pathways downstream of receptor tyrosine kinases such as EGFR, VEGFR, Her2, and PDGFR. A *pan*-Src kinase inhibitor

* To whom correspondence should be addressed. E-mail: jagabandhu.das@bms.com. Phone: 609-252-5068. Fax: 609-252-6804.

† Bristol-Myers Squibb Pharmaceutical Research Institute, Wallingford, CT.

[a] Abbreviations: Lck, lymphocyte-specific kinase; APC, antigen presenting cell; MHC, major histocompatability complex; TCR, T-cell antigen receptor; IL-2, interleukin 2; Abl, abelson tyrosine kinase; TNFα, tumor necrosis factor alpha; ITAM, immunoreceptor tyrosine activation motif; EGFR, epidermal growth factor receptor; VEGFR, vascular endothelial growth factor receptor; PDGFR, platelet derived growth factor receptor.

10.1021/jm060727j CCC: $33.50
Published on Web 10/24/2006

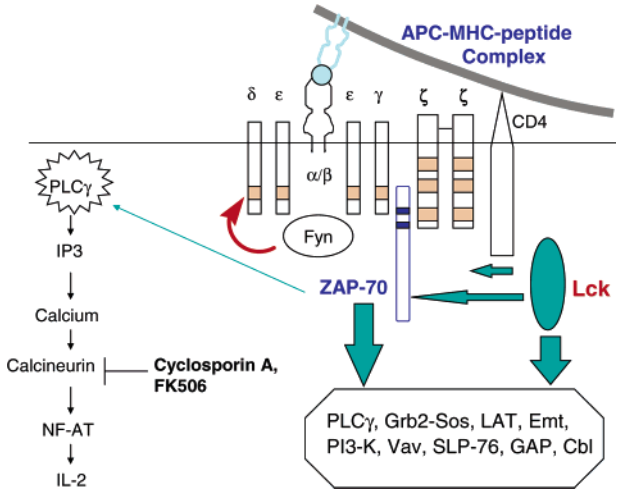

Figure 1. Schematic diagram of T-cell receptor (TCR) activation by antigen presenting cell (APC)—major histocompatibility peptide (MHC) complex.

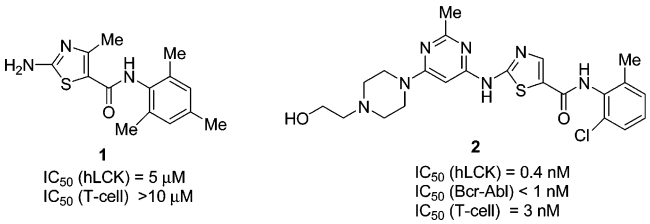

Figure 2. Activities of compounds **1** and **2**.

may be considered useful in modulating aberrant pathways leading to oncologic transformation of cells.

Screening of our internal compound collection using filter binding assays[11] identified aminothiazole **1** as an ATP competitive Lck inhibitor with a weak potency in biochemical and cell-based assays (murine Lck IC_{50} = 6.6 μM; human Lck IC_{50} = 5 μM; T-cell proliferation IC_{50} >10 μM)).[12] Subsequent structural modification through iterative structure−activity relationship (SAR) approaches led to the identification of extremely potent *pan*-Src inhibitors with picomolar activities against these enzymes. Within this class, several analogs also showed potent inhibitory activity against Bcr-Abl kinase. We describe here the synthesis, and SAR studies leading to the discovery of compounds **12m** and **2** (BMS-354825, dasatinib),[12c−e] as extremely potent *pan*-Src inhibitors (Figure 2).

Chemistry

Thiazole analogs described here were synthesized following the synthetic routes outlined in Schemes 1−3. To prepare the carboxamide, carbamate, and urea derivatives, appropriate 2-amino-thiazole-5-carboxylate **3** was treated with *di-tert*-butyl carbonate in the presence of 4-(*N*,*N*-dimethylamino)pyridine in THF to form the corresponding *tert*-butyl carbamate that upon saponification afforded the acid **4**. Conversion of the carboxylic acid to its acid chloride and its subsequent treatment with the appropriate aniline in the presence of diisopropylethylamine in dichloromethane or THF afforded the anilide **5**, which on further deprotection of the BOC-protecting group in TFA formed the aminothiazole **6**. Aminothiazole **6** served as an advanced intermediate for the synthesis of carboxamide, and ureido analogs. We utilized a solution-phase parallel synthesis approach to prepare a wide variety of such analogs. Accordingly, **6** was treated with a carboxylic acid chloride or its anhydride in the presence of an organic base to form amides **7**. Alternatively, **6** could be reacted with a carboxylic acid under standard peptide coupling conditions to form **7**. Reaction of **6** with an isocyanate in the presence of pyridine or 4-(*N*,*N*-dimethylamino)pyridine formed the urea analogs **9**. Compound **6** could also be converted to the phenyl carbamate **10**, which on further reaction with an amine in THF−acetonitrile mixture formed the urea **9**. Commercial availability of a wide variety of amines made the later approach more attractive for the synthesis of diverse urea analogs (Scheme 1).

The 2′-aminoheteroarylthiazole anilide analogs were prepared as described in Schemes 2 and 3. Ethyl 2-amino-thiazole-5-carboxylate (**3b**) was converted to amine **6b** following the synthetic sequence outlined in Scheme 1. Compound **6b** could be directly coupled to an activated heteroaromatic halide to form **12**. Alternatively, **6b** was treated with copper(II) bromide and *tert*-butyl nitrite in anhydrous degassed acetonitrile to form the bromide **18**, which on treatment with the appropriate heteroaryl amine and sodium hydride in THF afforded **12** (Scheme 2).

An alternate concise and efficient route was also developed for this series of analogs and is illustrated with the synthesis of **2** (Scheme 3). Treatment of 2-chlorothiazole **19** with *n*-butyllithium at −78 °C followed by addition of 2-chloro-6-methylphenyl isocyanate afforded anilide **14**. Protection of the anilide followed by reaction of **15** with 4-amino-6-chloro-2-methylpyrimidine in the presence of sodium hydride in THF and subsequent removal of the PMB protecting group formed **17**. Further homologation of **17** by treatment with 1-(2-hydroxyethyl)piperazine in dioxane afforded **2**, which was converted to its monohydrochloride salt with methanolic hydrogen chloride in ether.

Results and Discussion

Initial Structure−Activity Studies. Compounds were evaluated for their ability to inhibit Lck using both biochemical and cellular assays.[13] Our initial screening used recombinant mouse Lck (mLck) as the enzyme and enolase as substrate. Subsequently, mLck was substituted with recombinant human Lck (hLck). Because Lck shares a high degree of sequence homology (84%) between mouse and human, we reasoned this change will have an insignificant impact on the observed IC_{50} values, a hypothesis that was borne out by observation of a good correlation for a set of analogs (Tables 1 and 2).

Broad screening of our in-house compound collection identified aminothiazole **1** as a lead with weak biochemical potency against Lck and little cell activity up to a concentration of 10 μM. The corresponding *tert*-butyl carbamate **5a** was approximately equipotent and served as a starting point for further optimization. As part of a systematic SAR approach, we first investigated the importance of the carboxanilide side chain on the thiazole (Table 1). Substitution studies revealed an extremely narrow structural requirement at this position. Replacement of the 2,4,6-trimethyl substituents on the benzamide with hydrogen (**5f**) significantly attenuates potency. Both the 2-Me and 2,4-*di*-Me analogs (**5g** and **5j**) are also significantly less potent. The 2,6-*di*-Me analog (**5c**) is only 3-fold less potent. The 4-Me substituent can be replaced with bromo (**5d**) without loss of potency. Either or both of the *ortho*-methyl substituents on the benzamide can be replaced with a similarly small group (**5b** and **5e**) with minimal loss of potency. In contrast, substitution with sterically demanding groups (**5h** and **5i**) results in dramatic loss in potency. Overall, small substituents at both the *ortho* positions on the benzamide ring are optimal for Lck inhibitory

Scheme 1. Synthesis of Carboxamide, Carbamate, and Urea Analogs (**5** and **7**−**9**)[a]

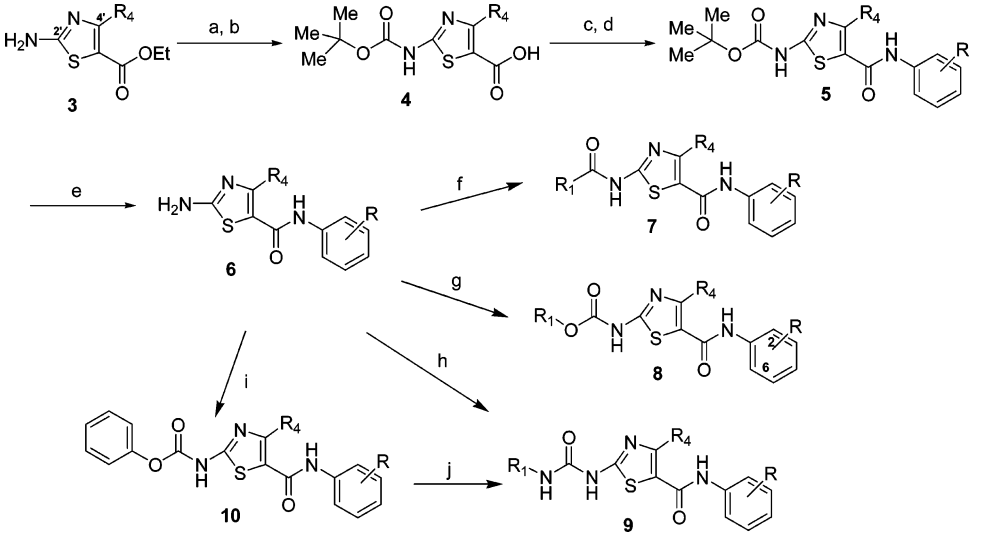

[a] Reagents and conditions: (a) BOC_2O, DMAP, THF, 70−72%; (b) NaOH, aq MeOH, 86−96%; (c) $(COCl)_2$, cat. DMF; (d) R-$PhNH_2$, *i*-Pr_2NEt, 28−100% in two steps; (e) TFA, rt, 68−100%; (f) R_1COCl or $(R_1CO)_2O$, THF, DMAP or R_1CO_2H, EDAC, HOBt, *i*-Pr_2NEt, 18−90%; (g) R_1OCOCl, aq $NaHCO_3$, THF, 75−85%; (h) R_1NCO, Py, 45−87%; (i) PhOCOCl, aq $NaHCO_3$, THF, 69−90%; (j) R_1NH_2, THF, CH_3CN, 75−95%.

Scheme 2. Synthesis of Heteroaryl Amines **12**[a]

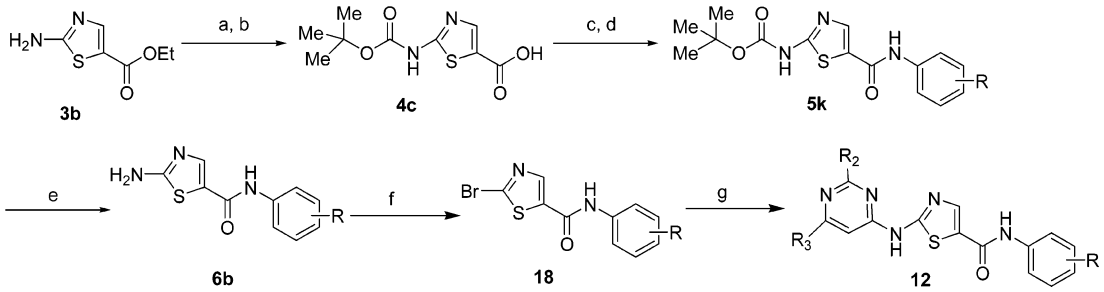

[a] Reagents and conditions: (a) BOC_2O, DMAP, THF, 70%; (b) NaOH, aq MeOH, 96%; (c) $(COCl)_2$, cat. DMF, CH_2Cl_2; (d) R-$PhNH_2$, CH_2Cl_2, *i*-Pr_2NEt; (e) TFA, rt, 19−85% in three steps; (f) $CuBr_2$, *t*-BuONO, CH_3CN, 69−78%; (g) R_2,R_3-4-amino-pyrimidine, THF, 60 °C, 19−70%.

Scheme 3. Synthesis of **2**[a]

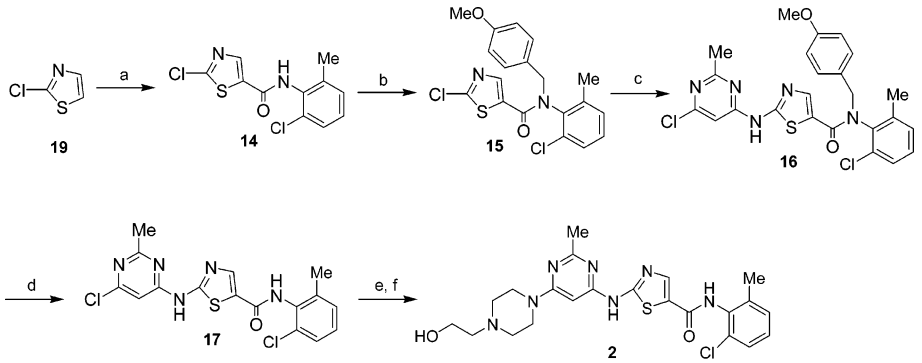

[a] Reagents and conditions: (a) *n*-BuLi, THF, 2-chloro-6-methylphenyl isocyanate, −78 °C, 86%; (b) NaH, 4-methoxybenzyl chloride, THF, 95%; (c) NaH, THF, 4-amino-6-chloro-2-methyl pyrimidine, Δ, 83%; (d) TfOH, TFA, CH_2Cl_2, 99%; (e) 1-(2-hydroxyethyl)piperazine, 1,4-dioxane, Δ; (f) HCl, Et_2O, MeOH, 91% in two steps.

activity of these analogs. This finding is consistent with similar observations with other classes of Lck inhibitors.[13,14] The *ortho* substituents are most likely required to orient the aniline ring out of the plane formed by the anilide and thiazole groups in order that it can fit into a narrow hydrophobic pocket of the enzyme (Table 1).[16]

Our attention turned next to the modification of the 2-amino substituent on the thiazole ring (Table 2). A large number of diverse carbamates, carboxamides, and ureas were prepared using a solution-phase parallel synthesis strategy. In general, derivatization of the amino group leads to improved Lck inhibitory activity in vitro. For example, the methyl carbamate (**7a**), acetamide (**7c**), and the methyl urea analogs (**8a**) are roughly 3−20-fold more potent than **1**. Sterically demanding groups in general lead to a significant loss in potency (**5a**, **7e**, and **8d**). Introduction of aryl and certain heteroaryl groups (**7d**, **7f**−**k**, **8b**, and **8e**) also led to significant enhancement in potency. In a direct comparison, the 2,4,6-trimethylaniline analogs (**7d**, **7f**, **7h**, and **8c**) are essentially equipotent to their 2-chloro-6-methylaniline counterparts (**7l**, **7k**, **7j**, and **8f**). *n*-Butyl urea **8c** was identified as the most potent inhibitor in this series (hLck IC_{50} = 30 nM).

Table 1. In Vitro Lck Activity of *tert*-Butoxycarbamate Analogs **5a**−**j**

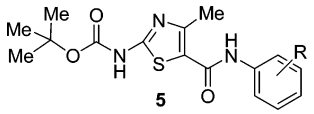

5

compd	R	mLck IC_{50}[a] (μM)	hLck IC_{50}[a] (μM)
5a	2,4,6-*tri*-Me	3	1.5
5b	2-Cl, 6-Me	9.6	28
5c	2,6-*di*-Me	7.5	4.4
5d	4-Br, 2,6-*di*-Me	2.4	1.4
5e	2,6-*di*-Cl		12.5
5f	H	28[b]	
5g	2-Me	45.7	
5h	2-Me, 6-*i*Pr	40.3	
5i	2-OMe, 6-Me	24.3	
5j	2,4-di-Me	27.4	

[a] $n = 3$, variation in individual values, <20%. [b] % inhibition @ 50 μM.

Table 2. In Vitro Lck Activity of 2-Amino-4-methyl-thiazole Analogs **7a**−**i** and **8a**−**f**

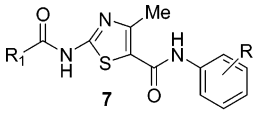

7

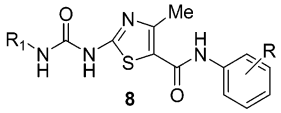

8

compd	R	R_1	mLck IC_{50}[a] (μM)	hLck IC_{50}[a] (μM)
7a	2,4,6-*tri*-Me	MeO−	0.72	0.7
7b	2,4,6-*tri*-Me	BnO−	33.32	
5a	2,4,6-*tri*-Me	*t*-BuO−	3	1.5
7c	2,4,6-*tri*-Me	Me	0.51	0.48
7d	2,4,6-*tri*-Me	Ph	0.32	0.8
7e	2,4,6-*tri*-Me	*t*-Bu		12.08
7f	2,4,6-*tri*-Me	2-furyl		0.36
7g	2,4,6-*tri*-Me	3-furyl		1.2
7h	2,4,6-*tri*-Me	3-thienyl		0.18
7i	2-Cl, 6-Me	3-thienyl		0.39
7j	2-Cl, 6-Me	2-thienyl		0.13
7k	2-Cl, 6-Me	2-furyl		0.71
7l	2-Cl, 6-Me	Ph		4.47
7m	2-Cl, 6-Me	cyclopropyl		1.4
8a	2,4,6-*tri*-Me	Me	0.17	0.24
8b	2,4,6-*tri*-Me	Ph	0.09	0.16
8c	2,4,6-*tri*-Me	*n*-Bu	0.07	0.03
8d	2,4,6-*tri*-Me	*t*-Bu		1.3
8e	2,4,6-*tri*-Me	Bn	0.10	0.13
8f	2-Cl, 6-Me	*n*-Bu		0.62

[a] $n = 3$, variation in individual values, <20%.

SAR studies were now directed toward modification of the substituent at the 4′-position of the thiazole. With a series of compounds in which the 2-amino group was functionalized as its *tert*-butyl carbamate derivative, we observed earlier that the replacement of the 4′-methyl substituent with several other groups (H, Et, Ph, and CF_3) led to significant attenuation in biochemical potency (hLck IC_{50}s > 30 μM). At this stage, our SAR findings in a related series prompted us to re-explore the 4′-substituent modification further. In a series of related benzothiazoles,[13a] introduction of a cyclopropyl amide at the 2′-position (**11**) leads to a dramatic increase in Lck biochemical potency (Figure 3). To our surprise, cyclopropyl amide analog **7n** (Table 3**)** with the 4′-unsubstituted thiazole core (hLck IC_{50} = 18 nM) is about 80-fold more potent than the corresponding 4′-methyl-substituted thiazole analog **7m** (hLck $IC_{50} = 1.4$ μM). This observation is in sharp contrast with our earlier findings in the *tert*-butyl carbamate series, where replacing the 4′-methyl by a hydrogen resulted in a significant loss in activity.[12a] Moreover, **7n** potently inhibits anti-CD3 and anti-CD28 induced

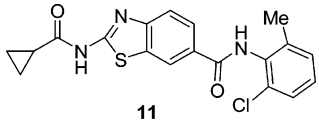

11

IC_{50} (hLCK) = 9 nM
IC_{50} (T-cell) = 4.7 μM

Figure 3. Activity of benzothiazole **11**.

Table 3. In Vitro Lck Activity of 2-Carboxamido-4-hydrido-thiazoles **7n**−**w**

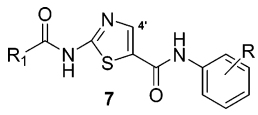

7

compd	R	R_1	hLck IC_{50}[a] (μM)
7n	2-Cl,6-Me	cyclopropyl	0.035
7o	2-Cl,6-Me	Et	*22*[b]
7p	2-Cl,6-Me	1-Me-cyclopropyl	*15*[b]
7q	2-Cl,6-Me	2-Me-cyclopropyl	*15*[b]
7r	2-Cl,6-Me	Ph	0.89
7s	2-Cl,6-Me	2-thienyl	2.23
7t	2-Cl,6-Me	3-thienyl	0.017
7u	2-Cl,6-Me	2-furyl	*29*[b]
7v	2-Cl,6-Me	cyclobutyl	*17*[b]
7w	2-Cl,6-Me	cyclopentyl	1.34

[a] $n = 3$, variation in individual values, <20%. [b] % inhibition @ 3.13 μM.

proliferation in a T-cell proliferation assay (IC_{50} = 884 nM). Further structural optimization was therefore focused on the 4′-unsubstituted thiazole core.

Table 3 summarizes the $C_{2'}$ carboxamide SAR. Replacement of the cyclopropyl amide with an alkyl (**7o**), cyclobutyl (**7v**) amide, or small alkyl substitution on the cyclopropyl ring (**7p**, **7q**) leads to a substantial loss (>1000-fold) in potency. Benzamide (**7r**), cyclopentyl amide (**7w**), and the 2-thienyl amide (**7s**) retains some of the intrinsic potency. Only the 3-thienyl amide **7t** displays comparable potency to **7n**. However, in the T-cell proliferation assay, **7t** ($IC_{50} > 2$ μM) is less potent than **7n**. Minor structural changes thus led to dramatic drops in activity, and as such, a very narrow SAR pattern was observed in this series.

Model of Aminothiazole Binding to Lck. Based on the published crystal structure of the ATP binding site of active, autophosphorylated Lck[15−17] and homology modeling based on a reported Hck structure,[18] we constructed an Lck binding site model, as described in our previous communications.[13,19] The binding model of **7n** highlights some of the critical H-bond interactions with the active site residues. The aniline NH appears to be positioned favorably for a productive hydrogen-bonding interaction with the Thr316 hydroxyl, and both the thiazole nitrogen and the cyclopropyl carboxamide NH are in H-bond contact with the backbone carbonyl and NH of Met319, respectively, at the hinge region of the protein. The cyclopropyl group appears to fit snugly in a hydrophobic pocket. This proposed binding mode is consistent with the 2,6-aniline disubstitution, which orients the phenyl ring so that it can fit into an angular deep but narrow hydrophobic pocket (Figure 4).

To rationalize the 4′-Me effect, we utilized the model structures shown in Figure 5. The preferred binding conformations for these compounds are represented by A1 and B1, respectively. When subjected to SAM 1d minimization, the 4′-unsubstituted thiazole was shown to adopt either conformation (A1 and A2) equally, while for the 4′-Me thiazole, the preferred

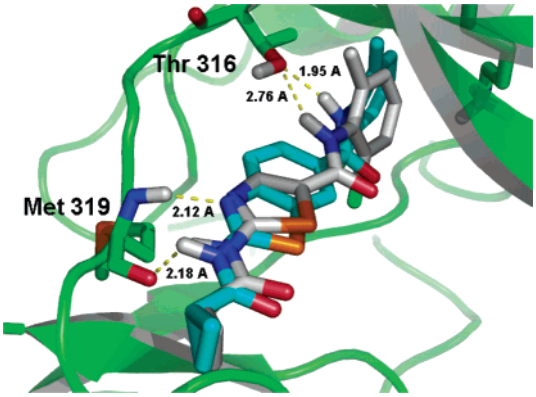

Figure 4. Proposed binding interactions of thiazole **7n** (white) and benzothiazole **11** (blue) with the Lck kinase.

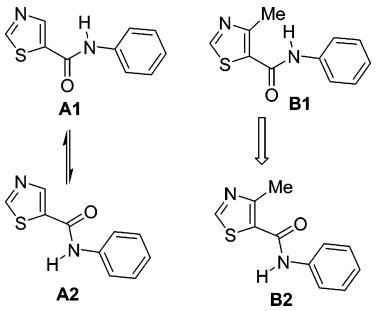

Figure 5. Proposed binding conformations of 4′-unsubstituted and 4′-Me thiazoles.

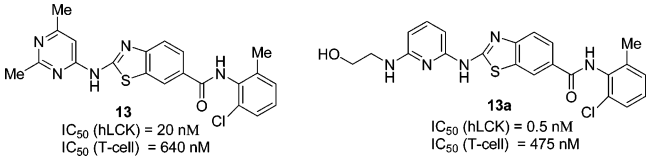

Figure 6. Activities of benzothiazoles **13** and **13a**.

conformation is B2. This conformation interferes with the ability of 4′-Me thiazole to adopt the required binding conformation and may explain the difference in biochemical potency observed between these series.

Heteroaryl Replacement of the 2′-Carboxamides and Identification of 2. Further SAR investigations with the benzothiazole Lck inhibitors revealed that replacement of the 2-carboxamide function with certain heteroaryl amines led to highly potent inhibitors (Figure 6).[13b] Molecular docking of **7n** (Figure 4) suggested that the cyclopropyl amide carbonyl was not engaged in any productive H-bond interaction. We, therefore, rationalized that the $C_{2'}$ carboxamide could be replaced with a heteroaryl amine that can function as a conformationally constrained "amide mimetic". These studies were, therefore, undertaken with the 4′-unsubstituted thiazole core (Table 4). Replacement of the $C_{2'}$ cyclopropyl carboxamide with a 2″-pyridyl amine (**12a**) leads to a 30-fold increase in biochemical potency and a 6-fold increase in cell potency. Regioisomeric 3″- and 4″-pyridyl analogs **12b** and **12c** are 6−8-fold less potent than the 2″-isomer. Similar improvements in both biochemical and cellular potencies were observed in the 2,6-*di*-Me and 2,4,6-*tri*-Me aniline series (**12d**,**e**). A wide variety of heterocyclic amine replacements (**12f**−**i**) were tolerated. Methyl substitution on the 2″-aminopyridine ring (**12j**,**k**) leads to a further enhancement in both in vitro enzyme and cellular activity. 4″,6″-Di-substitution on the pyridine ring (**12l**) is also tolerated. The 2″,6″-di-Me-4″-pyrimidinyl-substituted analog **12m** was identified as one of the more potent Lck inhibitors in this series. The

Table 4. In Vitro and Cell Activity of 2-Heteroarylamino-thiazoles **12a**−**o**

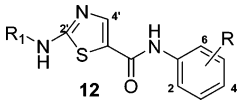

compd	R	R_1	hLck IC_{50}[a] (nM)	T-cell IC_{50}[b] (nM)
12a	2-Cl, 6-Me	2″-pyridyl	1.2	140
12b	2-Cl, 6-Me	3″-pyridyl	6.7	870
12c	2-Cl, 6-Me	4″-pyridyl	9.4	270
12d	2,6-*di*-Me	2″-pyridyl	1.2	180
12e	2,4,6-*tri*-Me	2″-pyridyl	5	510
12f	2-Cl, 6-Me	3″-pyridazinyl	4	350
12g	2,6-*di*-Me	3″-pyridazinyl	0.3	350
12h	2-Cl, 6-Me	3″,5″-*di*-Me-2″-pyrazinyl	6.3	570
12i	2,4,6-*tri*-Me	2″-pyrazinyl	4.9	500
12j	2-Cl, 6-Me	6″-Me-2″-pyridinyl	0.6	110
12k	2-Cl, 6-Me	4″-Me-2″-pyridinyl	0.5	80
12l	2-Cl, 6-Me	4″,6″-di-Me-2″-pyridinyl	4	140
12m	2-Cl, 6-Me	2″,6″-di-Me-4″-pyrimidinyl	1	80
12n	2-Cl, 6-Me	4″,6″-di-Me-2″-pyrimidinyl	50	
12o	2,4,6-*tri*-Me	2″,6″-di-Me-4″-pyrimidinyl	3	140

[a] $n = 3$, variation in individual values, <20%. [b] $n = 3$, variation in individual values, <30%.

corresponding analog **12o** in the 2,4,6-*tri*-Me aniline series is slightly less potent. Similarly, the regioisomeric pyrimidinyl analog **12n** is significantly less potent (50-fold) than **12m**, suggesting specific interactions of the heteroatoms in the active site binding pocket. Based on its substantial potency, **12m** (Lck K_i = 130 pM, T-cell IC_{50} = 80 nM) was selected for further characterization.

As in the benzothiazole series (Figure 6), further enhancements in both biochemical and cellular activities with the thiazoles are achieved through appending polar functional groups to the heteroaromatic ring (Table 5).[13b]

In the pyridine series, introduction of a weakly basic or polar residue at the 6″-position of the pyridine ring led to analogs (**12p**−**r**) with subnanomolar activities against Lck in vitro. Differentiation of these analogs at the biochemical level proved quite difficult because the IC_{50} values approached the enzyme concentration in this assay. More importantly, a 10−25-fold increase in cellular potency was observed with the morpholino and imidazolyl analogs **12q** and **12r**, respectively. A similar trend was observed with the pyrimidine-based analogs. Analogs having a morpholino group directly attached at the 2″-position of the pyrimidine (**12s**,**t**) or tethered through an alkylamino side chain (**12u**) displays nanomolar or below biochemical potency and single digit nanomolar activity in the T-cell assay. Finally, introduction of a 4-hydroxyethylpiperazinyl side chain at the 2″-position of the pyrimidine resulted in the identification of one of the most potent analogs (**2**) in the series. Compound **2** is roughly 30-fold more potent on T-cells than **12m**.

Characterization of 2′-(Heterocyclo)amino-thiazole Analogs. The proposed binding modes for **12m** and **2** (Figure 7) are consistent with that of the cyclopropyl amide **7n** (Figure 4) in that the key hydrogen-bond interactions of the pyrimidinyl NH, thiazole nitrogen, and the anilide NH are preserved. The critical requirement of the H-bond interactions of the pyrimidinyl and anilide NHs for Lck activity was demonstrated by synthesis

Table 5. In Vitro and Cell Activity of 2′-Heteroarylamino-thiazoles **2** and **12m**−**w**

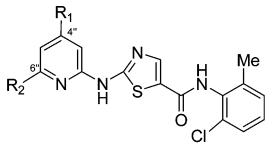

12p-r

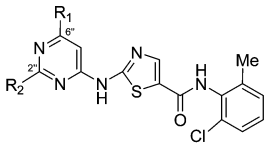

2, **12m**, and **12s-w**

compd	R_1	R_2	HLck IC_{50} (nM)[a]	T-cell IC_{50} (nM)[b]
12m	Me	Me	1	80
12p	H	-$NH(CH_2)_2OH$	<0.2	75
12q	H	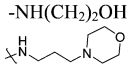	0.5	8
12r	H	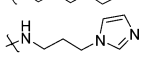	<0.5	2
12s		H	0.5	3
12t		Me	1.3	5
12u	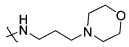	Me	0.7	7
12v	-$NH(CH_2)_2OH$	Me	0.2	23
12w	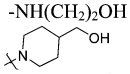	Me	0.7	4
2	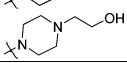	Me	0.4	3

[a] $n = 3$, variation in individual values, <20%. [b] $n = 3$, variation in individual values, <30%.

of the corresponding N−Me derivatives, both of which are significantly less potent than the parent **12m**.[12b] A similar attenuation in biochemical activity is observed with other thiazole analogs.[12a] Furthermore, as illustrated with **12m** (left, inset), the 2-amino pyrimidine ring appears to occupy a relatively narrow hydrophobic pocket delineated by Leu251, Tyr318, and Gly322. This may explain the increased binding affinity of the heteroaryl amine analogs in comparison to amides, carbamates, and ureas. The polar 4-hydroxyethylpiperazine residue in **2** approaches the solvent front and does not appear to engage in additional H-bond interactions. The significant increase in cellular potency of **2** and related analogs relative to **12m** cannot be readily explained by our binding model nor is it likely to be solely attributed to improvement of the physicochemical properties and/or cell permeability due to incorporation of a polar side chain. Nevertheless, **2** was identified as one of the most potent Lck inhibitors in the T-cell proliferation assay. It is also possible that the Lck construct used in the biochemical assay is not a perfect reflection of the enzyme in cells.

To better understand their enzyme inhibitor properties, both **2** and **12m** were evaluated for their selectivity against a panel of in-house kinases, some of which are shown in Table 6. Compound **12m** was a potent inhibitor of all Src family kinases and Bcr-Abl kinase. A high degree of selectivity (>200 fold) was observed against other tyrosine and serine/threonine kinases. A similar selectivity profile was observed with **2**, which strongly inhibited the Src family kinases Lck, Src, Yes, Fyn, c-kit, and Bcr-Abl kinase with subnanomolar potencies. Analog **2** was also highly selective against other kinases tested. Compounds **2** and **12m** were further confirmed to be potent ATP competitive inhibitors of Lck and Src with K_i values of 130 pM and 96 pM, respectively, for **12m** and 64 pM and 16 pM, respectively, for **2**. In addition, **2** was a highly potent ATP competitive inhibitor of Bcr-Abl ($K_i = 30 \pm 22$ pM). The lack of selectivity of these analogs over other Src family kinases is not unexpected, because the kinase domain is known to be highly conserved among its members. In addition, the structural similarities of Lck and activated Abl kinase may explain the strong inhibition of the Bcr-Abl kinase by these analogs.[20]

Efficacy of compound **12m** was evaluated ex vivo in a mouse anti-CD3/anti-CD28 induced IL-2 production model. When dosed orally 2 h prior to anti-CD3/anti-CD28 stimulation, compound **12m** reduced serum IL-2 level in a dose-dependent manner with an ED_{50} value of approximately 5 mg/kg (Figure 8).

Compound **12m** was further characterized in vivo in an acute murine model of LPS-induced TNFα. Overproduction of TNFα, a major proinflammatory cytokine is implicated in several inflammatory diseases.[21] The blockade of TNFα function by anti-TNFα biologics such as Enbrel (Etanercept), Remicade (Infliximab), and Humira is demonstrated to be clinically efficacious in the treatment of RA, Crohn's disease, and psoriasis.[22] When dosed orally 2 h prior to LPS challenge, **12m** inhibited TNFα production in a dose-dependent manner (Figure 9). Statistically significant inhibition of TNF production (90%) was observed at an oral dose of 60 mg/kg. This reduction in TNF production may be attributed to the inhibition of Src family kinases Hck and Fgr, which regulate TNFα production by monocytes and macrophages. Inhibition of p38 kinase ($IC_{50} =$ 202 nM) may also contribute to the inhibition of TNF production by this analog. Compound **12m**, a potent inhibitor of both these kinases (Hck $IC_{50} = 2$ nM, Fgr $IC_{50} = 0.8$ nM) inhibited LPS-induced TNFα production in human peripheral blood mononuclear cells (PBMC) with an IC_{50} value of 670 nM.

The in vivo pharmacokinetic profile of **12m** was determined in rats. Upon administration of single doses of 10 mg/kg (iv and po), compound **12m** had a peak plasma exposure of 2 μM (C_{max}) with a T_{max} of 1 h. Both plasma half-life ($t_{1/2}$) and mean residence time were approximately 4 h. Compound **12m** had a moderate rate of plasma clearance (29 mL/min/kg) and a large volume of distribution (Vsss = 12 L/kg), indicative of wide tissue distribution. Oral bioavailabilty of **12m** in rats was determined to be 65%.

T-cell activation is known to play a critical role in the pathogenesis of RA.[23] Recent studies demonstrating the clinical efficacy of CTLA4-Ig, an inhibitor of the T-cell costimulation, in RA patients has validated the strategy of blocking T-cell activation for the treatment of RA.[24] Because Lck plays a central role in T-cell activation in response to antigen, we evaluated the anti-inflammatory efficacy of **12m** in a rat adjuvant arthritis model of established disease, which is a widely utilized model of human RA. Furthermore, this model was chosen based on acceptable pharmacokinetic profile, including oral bioavailability of **12m** in rats. In this model, male Lewis rats were immunized with complete Freund's adjuvant at the base of the tail and hind paw volumes were measured to assess disease progression. Rats were treated with **12m** or vehicle beginning on day 14 after immunization when arthritic disease was well-established. As shown in Figure 10, **12m** significantly reduced the progression of paw swelling when administered orally at 0.3 and 3 mg/kg twice daily.

Conclusion

Our broad screening effort identified the 2′-amino-4′methyl thiazole **1** as a novel Lck inhibitor. Iterative SAR studies showed the 4′-unsubstituted-2′-amino thiazole to be an optimal template for Src family kinase inhibition. Further structural refinements on the 4′-unsubstituted thiazole core based on insights from SAR studies in a related series of benzothiazoles led to the discovery of analogs **2** and **12m** as highly potent *pan*-Src kinase inhibitors. In addition, using molecular modeling, we developed a putative

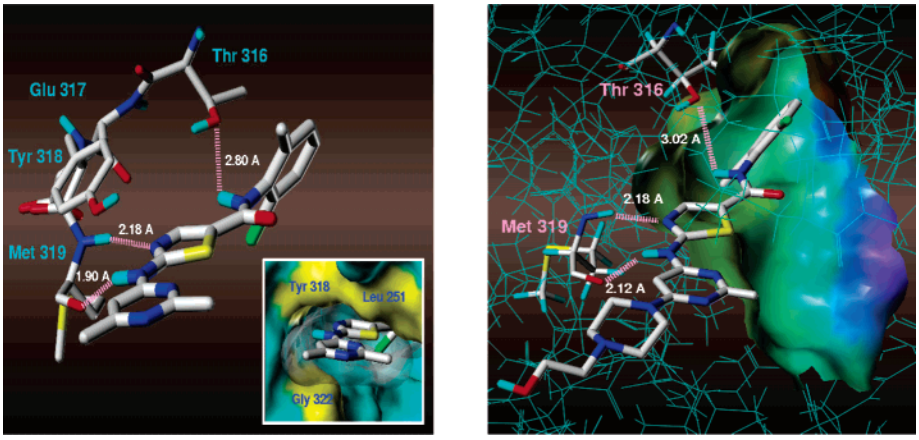

Figure 7. Proposed binding interactions of **12m** (left) and **2** (right) with the Lck kinase domain. Van der waals surfaces are shown for **12m** (left, inset).

Table 6. Kinase Selectivity Profiles of **2** and **12m**

compd	Lck IC_{50} (nM)	Src IC_{50} (nM)	Fyn IC_{50} (nM)	Hck IC_{50} (nM)	Yes IC_{50} (nm)	Lyn IC_{50} (nM)	Bcr-Abl IC_{50} (nM)	Cdk2 IC_{50} (nM)	p38 IC_{50} (nM)	Her1 IC_{50} (nM)	Her2 IC_{50} (nM)	FGFR1 IC_{50} (nM)
2	0.4	0.5	0.2		0.5		<1	>5000	100	180	710	880
12m	1	<2	1	2	2	4	3	>25 000	202	5200	500	>10 000

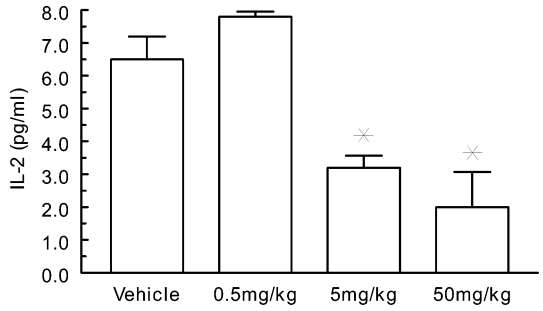

Figure 8. Inhibition of anti-CD3/anti-CD28 stimulated IL-2 production ex vivo in mice (n = 7/group, mean ± SEM) by compound **12m** (*p < 0.01).

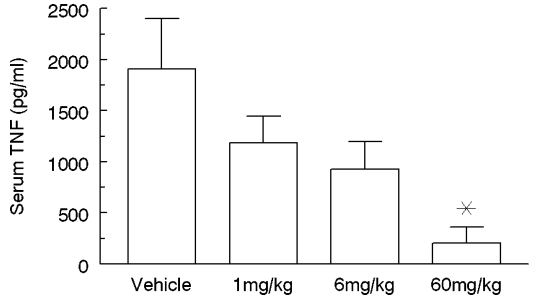

Figure 9. Inhibition of LPS-induced TNFα induction in mice (n = 11−12/group, mean ± SEM). Compound **12m** was dosed orally 2 h prior to LPS challenge (*p < 0.01).

binding model for Lck inhibition by this class of compounds. The framework of key hydrogen-bond interactions proposed by this model is in agreement with the subsequent, published crystal structure of **2** bound to the structurally similar Abl kinase.[12c] The oral efficacy of this class of inhibitors was demonstrated with **12m** in inhibiting the proinflammatory cytokine IL-2 ex vivo in mice and in reducing TNF levels in an acute murine model of inflammation. The oral efficacy of **12m** was further demonstrated in a chronic model of adjuvant arthritis in rats with established disease when administered orally at 0.3 and 3 mg/kg twice daily. Our research culminated in the identification of **2** as an exquisitely potent inhibitor of the Src family kinases.

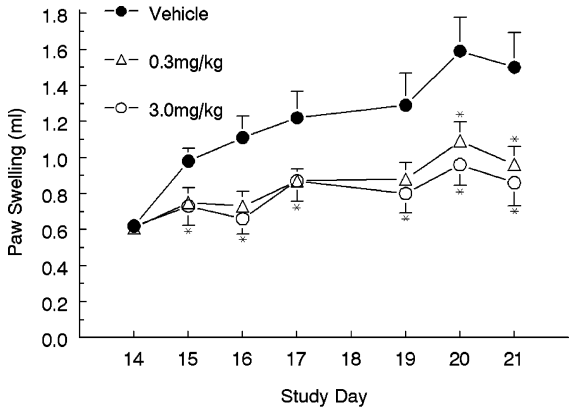

Figure 10. Efficacy of compound 12**m** in the treatment of rats with established adjuvant arthritis disease: mean ± SEM, n = 8/group.

As reported earlier,[12c] compound **2** is currently in clinical trials[25] for the treatment of chronic myelogenous leukemia.

Experimental Section

Chemistry. All solvents and reagents were obtained from commercial sources and used without further purification unless noted otherwise. Proton and carbon magnetic resonance (^{1}H and ^{13}C NMR) spectra were recorded on one of the following instruments: CPF-270 spectrometer operating at 270 or 67.5 MHz, Bruker AVANCE 400 MHz, Bruker DRX-400 MHz, JEOL ECL-500 MHz, JEOL ECL-400 MHz spectrometer and chemical shifts are reported in ppm (δ) from the tetramethylsilane resonance in the indicated solvent. High-resolution mass spectra (HRMS) were recorded on a JEOL SX102 mass spectrometer. Flash chromatography was carried out on E. Merck Kieselgel 60 silica gel (230−400 mesh). Elemental analyses were performed by Robertson Microlit Laboratories, and the results are within ±0.4% of the theoretical value, unless indicated otherwise. Analytical HPLC and LC/MS analyses were conducted using a Shimadzu LC-10AS liquid chromatograph and a SPD-10AVUV-vis detector at 220 nm with the MS detection performed with a Micromass Platform LC spectrometer. HPLC and LC/MS methods are detailed below. Preparative reverse-phase HPLC purifications were performed using the following conditions: Ballistic YMC S5 ODS 20 × 100 mm column or 30 × 250 mm with a binary solvent system where solvent

A = 10% methanol, 90% water, 0.1% trifluoroacetic acid and solvent B = 90% methanol, 10% water, and 0.1% trifluoroacetic acid, flow rate = 20 mL/min, linear gradient time = 10 min, start % B = 20, final % B = 100.

HPLC Methods. Method A. A linear gradient program using 10% methanol, 90% water, and 0.2% H_3PO_4 (solvent A) and 90% methanol, 10% water, and 0.2% H_3PO_4 (solvent B); $t = 0$ min, 0% B, $t = 4$ min, 100% B was employed on a YMC S5 ODS 4.6 × 50 mm Ballastic column. Flow rate was 4 mL/min, and UV detection was set to 220 nm. The LC column was maintained at ambient temperature.

Method B. A linear gradient program using 10% methanol, 90% water, and 0.2% H_3PO_4 (solvent A) and 90% methanol, 10% water, and 0.2% H_3PO_4 (solvent B); $t = 0$ min, 0% B, $t = 30$ min, 100% B was employed on a Zorbax S8 C18 4.5 × 75 mm column. Flow rate was 2.5 mL/min, and UV detection was set to 217 nm. The LC column was maintained at ambient temperature.

Method C. A linear gradient program using 10% methanol, 90% water, and 0.2% H_3PO_4 (solvent A) and 90% methanol, 10% water, and 0.2% H_3PO_4 (solvent B); $t = 0$ min, 0% B, $t = 8$ min, 100% B was employed on a YMC OCD 4.6 × 50 mm column. Flow rate was 2.5 mL/min, and UV detection was set to 220 nm. The LC column was maintained at ambient temperature.

Method D. A linear gradient program using 10% methanol, 90% water, and 0.1% TFA (solvent A) and 90% methanol, 10% water, and 0.1% TFA (solvent B); $t = 0$ min, 0% B, $t = 4$ min, 100% B was employed on a YMC Combiscreen 4.6 × 50 mm S-5 column. Flow rate was 4 mL/min, and UV detection was set to 220 nm. The LC column was maintained at ambient temperature.

Method E. A linear gradient program using 10% methanol, 90% water, and 0.2% H_3PO_4 (solvent A) and 90% methanol, 10% water, and 0.2% H_3PO_4 (solvent B); $t = 0$ min, 0% B, $t = 30$ min, 100% B was employed on a YMC S-3 ODS 6 × 150 mm column. Flow rate was 1.5 mL/min, and UV detection was set to 217 nm. The LC column was maintained at ambient temperature.

Method F. A linear gradient program using 10% methanol, 90% water, and 0.2% H_3PO_4 (solvent A) and 90% methanol, 10% water, and 0.2% H_3PO_4 (solvent B); $t = 0$ min, 0% B, $t = 4$ min, 100% B was employed on a YMC C18 S5 4.6 × 50 mm Ballastic column. Flow rate was 3 mL/min, and UV detection was set to 220 nm. The LC column was maintained at ambient temperature.

Ethyl-2-[[(*tert*-butyloxy)carbonyl]-amino]-4-methyl-1,3-thiazole-5-carboxylate (4a): A solution of ethyl 2-amino-4-methylthiazole-5-carboxylate (**3a**, 18.6 g, 100 mmol), di-*tert*-butyl carbonate (26.2 g, 120 mmol), and catalytic 4-dimethylamino pyridine (800 mg, 6.6 mmol) in dry THF (300 mL) was stirred under an inert atmosphere for 18 h. The reaction mixture was concentrated. The residue was suspended in dichloromethane (1 L) and filtered through a pad of Celite. The filtrate was washed with 1 N aq HCl solution, water, and brine, dried ($MgSO_4$), filtered, and concentrated. The residue was triturated with hexanes. The solid was filtered and dried in vacuo to obtain **4a** (20 g, 72%) as a solid. ^{1}H NMR (270 MHz, $CDCl_3$) δ 11.03 (br s, 1H), 4.3 (q, $J = 7.3$ Hz, 2H), 2.67 (s, 3H), 1.55 (s, 9H), 1.35 (t, $J = 7.3$ Hz, 3H). ^{13}C NMR ($CDCl_3$) δ 163.3, 162.6, 156.3, 152.5, 114.7, 83.5, 60.8, 28.2, 17.0, 14.3.

2-[[(*tert*-Butyloxy)carbonyl]-amino]-4-methyl-1,3-thiazole-5-carboxylic Acid (4b): A solution of **4a** (10 g, 34.95 mmol) in THF−EtOH (250 mL, 2:3) and 6 N aq KOH solution (250 mL) was heated to 55 °C overnight under an inert atmosphere. The solution was cooled to 0 °C and acidified with concd HCl to pH 1. The solution was concentrated in vacuo, and the residue was washed with water, ether, and dried in vacuo over P_2O_5 to obtain **4b** (89%) as a white solid. ^{1}H NMR (270 MHz, DMSO-d_6) δ 2.52 (s, 3H), 1.40 (s, 9H). ^{13}C NMR (DMSO-d_6) δ 163.6, 161.2, 155.8, 152.7, 115.0, 81.8, 27.8, 16.9.

2-[[(*tert*-Butyloxy)carbonyl]-amino]-4-methyl-*N*-(2,4,6-trimethylphenyl)-1,3-thiazole-5-carboxamide (5a): A 2 M solution of oxalyl chloride (22.5 mL, 45 mmol) in dichloromethane was added dropwise to a stirred suspension of **4b** (10 g, 38.7 mmol) and DMF (150 μL) in dichloromethane at 0 °C. The solution was warmed to room temperature, stirred for 1.5 h, and concentrated. The residue was azeotroped with toluene (300 mL, 2×) and dried in vacuo to obtain the crude acid chloride (10.7 g, 99%) as a tan solid.

2,4,6-Trimethylaniline (6.3 mL, 44.9 mmol) was added slowly to a stirred solution of crude acid chloride (10.7 g, 38.7 mmol) in dichloromethane (150 mL) at 0 °C. After 20 min, diisopropylethylamine (88 mL, 50.7 mmol) was added dropwise. The solution was warmed to room temperature and stirred for 2 h. The solution was concentrated. The residue was suspended in EtOAc (700 mL), washed with 1 N aq HCl solution, water, and brine. The EtOAc extract was separated, dried ($MgSO_4$), filtered, and concentrated. The residue was triturated with EtOAc to obtain **5a** (12.5 g, 86%) as a tan solid. ^{1}H NMR (400 MHz, DMSO-d_6) δ 11.71 (s, 1H), 9.15 (s, 1H), 6.89 (s, 2H), 2.53 (s, 3H), 2.23 (s, 3H), 2.11 (s, 6H), 1.48 (s, 9H). HRMS (ESI) *m*/*z* calcd for $C_{19}H_{26}N_3O_3S$ $[M + H]^+$, 376.1697; found, 376.1690. Purity: 100% (method C; $t_R = 7.71$ min), 100% (method E; $t_R = 31.35$ min).

2-[[(*tert*-Butyloxy)carbonyl]-amino]-4-methyl-*N*-(2-chloro-6-methylphenyl)-1,3-thiazole-5-carboxamide (5b): ^{1}H NMR (400 MHz, DMSO-d_6) δ 11.74 (s, 1H), 9.51 (s, 1H), 7.37 (dd, $J = 7.63$, 2.03 Hz, 1H), 7.20−7.28 (m, 2H), 2.56 (s, 3H), 2.21 (s, 3H), 1.49 (s, 9H). HRMS (ESI) *m*/*z* calcd for $C_{17}H_{21}ClN_3O_3S$ $[M + H]^+$, 382.0993; found, 382.1001. Purity: >99% (method A; $t_R = 3.86$ min), 100% (method D; $t_R = 3.29$ min).

2-[[(*tert*-Butyloxy)carbonyl]-amino]-4-methyl-*N*-(2,6-dimethylphenyl)-1,3-thiazole-5-carboxamide (5c): ^{1}H NMR (400 MHz, DMSO-d_6) δ 11.69 (s, 1H), 9.23 (s, 1H), 7.09 (s, 3H), 2.48 (s, 3H), 2.16 (s, 6H), 1.49 (s, 9H). HRMS (ESI) *m*/*z* calcd for $C_{18}H_{24}N_3O_3S$ $[M + H]^+$, 362.1539; found, 362.1544. Purity: 100% (method A; $t_R = 3.87$ min), 98% (method D; $t_R = 3.26$ min).

2-[[(*tert*-Butyloxy)carbonyl]-amino]-4-methyl-*N*-(4-bromo-2,6-dimethylphenyl)-1,3-thiazole-5-carboxamide (5d): ^{1}H NMR (400 MHz, DMSO-d_6) δ 11.73 (s, 1H), 9.27 (s, 1H), 7.32 (s, 2H), 2.47 (s, 3H), 2.15 (s, 6H), 1.48 (s, 9H). HRMS (ESI) *m*/*z* calcd for $C_{18}H_{23}BrN_3O_3S$ $[M + H]^+$, 440.0644; found, 440.0633. Purity: >99% (method A; $t_R = 4.24$ min), 93% (method D; $t_R = 3.44$ min).

2-[[(*tert*-Butyloxy)carbonyl]-amino]-4-methyl-*N*-phenyl-1,3-thiazole-5-carboxamide (5f): ^{1}H NMR (400 MHz, DMSO-d_6) δ 11.77 (s, 1H), 9.88 (s, 1H), 7.67 (d, $J = 7.6$ Hz, 2H), 7.33 (t, $J = 7.6$ Hz, 2H), 7.09 (t, $J = 7.4$ Hz, 1H), 2.49 (s, 3H), 1.51 (s, 9H). HRMS (ESI) *m*/*z* calcd for $C_{16}H_{20}N_3O_3S$ $[M + H]^+$, 334.1226; found, 334.1239. Purity: 98% (method D; $t_R = 3.18$ min), >92% (method E; $t_R = 29.5$ min).

2-[[(*tert*-Butyloxy)carbonyl]-amino]-4-methyl-*N*-(2-methylphenyl)-1,3-thiazole-5-carboxamide (5g): ^{1}H NMR (400 MHz, DMSO-d_6) δ 11.71 (s, 1H), 9.38 (s, 1H), 7.33 (d, $J = 7.63$ Hz, 1H), 7.24 (d, $J = 7.63$ Hz, 1H), 7.18 (t, $J = 7.63$ Hz, 1H), 7.13 (t, $J = 7.63$ Hz, 1H), 2.53 (s, 3H), 2.21 (s, 3H), 1.49 (s, 9H). HRMS (ESI) *m*/*z* calcd for $C_{17}H_{22}N_3O_3S$ $[M + H]^+$, 348.1387; found, 348.1397. Purity: >95% (method A; $t_R = 3.87$ min), 98% (method D; $t_R = 3.11$ min).

2-[[(*tert*-Butyloxy)carbonyl]-amino]-4-methyl-*N*-(2-isopropyl-6-methylphenyl)-1,3-thiazole-5-carboxamide (5h): ^{1}H NMR (400 MHz, DMSO-d_6) δ 11.70 (s, 1H), 9.24 (s, 1H), 7.13−7.24 (m, 2H), 7.09 (dd, $J = 6.61$, 2.03 Hz, 1H), 3.10 (m, 1H), 2.47 (s, 3H), 2.15 (s, 3H), 1.49 (s, 9H), 1.12 (d, $J = 5.09$ Hz, 6H). HRMS (ESI) *m*/*z* calcd for $C_{20}H_{28}N_3O_3S$ $[M + H]^+$, 390.1852; found, 390.1851. Purity: >95% (method A; $t_R = 4.17$ min), >95% (method D; $t_R = 3.44$ min).

2-[[(*tert*-Butyloxy)carbonyl]-amino]-4-methyl-*N*-(2-methoxy-6-methylphenyl)-1,3-thiazole-5-carboxamide (5i): ^{1}H NMR (400 MHz, DMSO-d_6) δ 11.65 (s, 1H), 9.00 (s, 1H), 7.16 (t, $J = 7.9$ Hz, 1H), 6.88 (d, $J = 7.9$ Hz, 1H), 6.83 (d, $J = 7.9$ Hz, 1H), 3.73 (s, 3H), 2.47 (s, 3H), 2.14 (s, 3H), 1.48 (s, 9H). MS (ESI) *m*/*z* 378 $[M + H]^+$. Purity: 100% (method A; $t_R = 3.79$ min), 96% (method D; $t_R = 3.17$ min).

2-[[(*tert*-Butyloxy)carbonyl]-amino]-4-methyl-*N*-(2,4-dimethylphenyl)-1,3-thiazole-5-carboxamide (5j): ^{1}H NMR (400 MHz, DMSO-d_6) δ 11.68 (s, 1H), 9.30 (s, 1H), 7.18 (d, $J = 8.1$ Hz, 1H), 7.04 (s, 1H), 6.98 (d, $J = 8.1$ Hz, 1H), 2.53 (s, 3H), 2.26 (s, 3H),

2.16 (s, 3H), 1.48 (s, 9H). HRMS (ESI) *m*/*z* calcd for $C_{18}H_{24}N_3O_3S$ $[M + H]^+$, 362.1539; found, 362.1544. Purity: 95% (method A; $t_R = 4.05$ min), 95% (method D; $t_R = 3.43$ min).

2-Amino-4-methyl-*N*-(2,4,6-trimethylphenyl)-1,3-thiazole-5-carboxamide (1). A solution of **5a** (10 g, 26.6 mmol) in trifluoroacetic acid (100 mL) was stirred at 0 °C for 3 h. The solution was concentrated, diluted with EtOAc, and washed with 5% aq $KHCO_3$ solution, water, and brine. The EtOAc extract was separated, dried ($MgSO_4$), filtered, and concentrated. The residue was rinsed with EtOAc (200 mL) and AcCN (100 mL) and dried in vacuo to obtain **1** (91%) as a white solid. ^{1}H NMR (270 MHz, DMSO-d_6) δ 8.68 (s, 1H), 7.38 (s, 2H), 6.9 (s, 2H), 4.88 (s, 2H), 2.39 (s, 3H), 2.22 (s, 3H), 2.20 (s, 6H). ^{13}C NMR (DMSO-d_6) δ 167.9, 160.6, 153.8, 135.5, 132.9, 128.2, 112.0, 20.5, 18.1, 17.2. Anal. Calcd for $C_{14}H_{17}N_3OS \cdot 0.15H_2O$: C, 60.47; H, 6.27; N, 15.11; S, 11.53. Found: C, 60.45; H, 6.19; N, 15.01; S, 11.61. Purity: 100% (method C; $t_R = 4.77$ min).

2-[[(Methoxy)carbonyl]-amino]-4-methyl-*N*-(2,4,6-trimethylphenyl)-1,3-thiazole-5-carboxamide (7a): A solution of **1** (100 mg, 0.36 mmol), methyl chloroformate (111 μL, 1.44 mmol), and pyridine (87 μL, 1.08 mmol) in dichloromethane (3 mL) was stirred at rt for 1.5 h. The solution was diluted with dichloromethane, washed with aq $NaHCO_3$ solution, and brine. Dichloromethane extract was separated, dried ($MgSO_4$), filtered, and concentrated. The residue was triturated with ether and dried in vacuo to obtain **7a** (88 mg, 82%) as a white solid. ^{1}H NMR (400 MHz, DMSO-d_6) δ 11.99 (s, 1H), 9.18 (s, 1H), 6.90 (s, 2H), 3.75 (s, 3H), 2.50 (s, 3H), 2.23 (s, 3H), 2.12 (s, 6H). HRMS (ESI) *m*/*z* calcd for $C_{16}H_{20}N_3O_3S$ $[M + H]^+$, 334.0564; found, 334.1225. Purity: 100% (method E; $t_R = 25.68$ min).

2-[[(Benzyloxy)carbonyl]-amino]-4-methyl-*N*-(2,4,6-trimethylphenyl)-1,3-thiazole-5-carboxamide (7b): ^{1}H NMR (270 MHz, DMSO-d_6) δ 12.2 (br s, 1H), 9.21 (s, 1H), 7.43 (m, 5H), 6.91 (s, 2H), 5.25 (s, 2H), 2.5 (s, 3H), 2.24 (s, 3H), 2.13 (s, 6H). HRMS (ESI) *m*/*z* calcd for $C_{22}H_{24}N_3O_3S$ $[M + H]^+$, 410.1540; found, 410.1537. Purity: 98% (method B, gradient time 8 min; $t_R = 8.66$ min).

2-[[(*tert*-Butyl)carbonyl]-amino]-4-methyl-*N*-(2,4,6-trimethylphenyl)-1,3-thiazole-5-carboxamide (7e): A solution of **1** (30 mg, 0.11 mmol), *tert*-butylacetic acid (13.3 mg, 0.13 mmol), HOBt (19.5 mg, 0.14 mmol), EDAC (26.8 mg, 0.14 mmol), and diisopropylethyl amine (60 μL, 0.34 mmol) in THF (400 μL) was heated to 45 °C in a sealed tube for 24 h. The mixture was diluted with CH_2Cl_2 and washed with 2 N aq HCl solution. The CH_2Cl_2 solution was passed through a Varian SCX cation exchange column on a Gilson robot. The column was eluted sequentially with CH_3CN-MeOH (10 mL, 4:1), 1.5 M methanolic NH_3 solution (3 mL), and 2 M methanolic NH_3 solution (3 mL, 4×). Fractions containing the product were concentrated in vacuo to obtain **7e** (30 mg, 77%). ^{1}H NMR (270 MHz, DMSO-d_6) δ 9.2 (s, 1H), 6.9 (s, 2H), 2.55 (s, 3H), 2.25 (s, 3H), 2.14 (s, 6H), 1.25 (s, 9H). HRMS (ESI) *m*/*z* calcd for $C_{19}H_{25}N_3O_2S$ $[M + H]^+$, 360.1748; found, 360.1751. Purity: 100% (method B; $t_R = 8.3$ min).

2-[(Benzoyl)amino]-4-methyl-*N*-(2,4,6-trimethylphenyl)-1,3-thiazole-5-carboxamide (7d): ^{1}H NMR (270 MHz, $CDCl_3$) δ 10.22 (br s, 1H), 7.95 (d, 2H), 7.65 (t, 1H), 7.55 (t, 2H), 6.9 (m, 3H), 2.6 (s, 3H), 2.25 (s, 3H), 2.2 (s, 6H). HRMS (ESI) *m*/*z* calcd for $C_{21}H_{22}N_3O_2S$ $[M + H]^+$, 380.1432; found, 380.1420. Purity: >95% (method E; $t_R = 29.8$ min).

2-[[(Furanyl)carbonyl]-amino]-4-methyl-*N*-(2,4,6-trimethylphenyl)-1,3-thiazole-5-carboxamide (7f): ^{1}H NMR (270 MHz, $CDCl_3$) δ 7.62 (s, 1H), 7.42 (d, $J = 3.5$ Hz, 1H), 6.94 (s, 2H), 6.89 (br s, 1H), 6.64 (m, 1H), 2.7 (s, 3H), 2.29 (s, 3H), 2.25 (s, 6H). MS (ESI) *m*/*z* 370 $[M + H]^+$. Purity: 93% (method A; $t_R = 4.45$ min).

3-[[(Furanyl)carbonyl]-amino]-4-methyl-*N*-(2,4,6-trimethylphenyl)-1,3-thiazole-5-carboxamide (7g): ^{1}H NMR (400 MHz, DMSO-d_6) δ 12.69 (br s, 1H), 9.3 (s, 1H), 8.61 (s, 1H), 7.87 (s, 1H), 7.12 (s, 1H), 6.93 (s, 2H), 2.54 (s, 3H), 2.25 (s, 3H), 2.15 (s, 6H).). HRMS (ESI) *m*/*z* calcd for $C_{19}H_{20}N_3O_3S$ $[M + H]^+$, 370.1226; found, 370.1209. Purity: 100% (method A; $t_R = 4.54$ min).

3-[[(Thienyl)carbonyl]-amino]-4-methyl-*N*-(2,4,6-trimethylphenyl)-1,3-thiazole-5-carboxamide (7h): ^{1}H NMR (400 MHz, DMSO-d_6) δ 12.76 (s, 1H), 9.3 (s, 1H), 8.65 (s, 1H), 7.74 (d, $J = 5.09$ Hz, 1H), 7.7 (m, 1H), 6.93 (s, 2H), 2.59 (s, 3H), 2.26 (s, 3H), 2.16 (s, 6H). HRMS (ESI) *m*/*z* calcd for $C_{19}H_{20}N_3O_2S_2$ $[M + H]^+$, 386.0999; found, 386.1008. Purity: 100% (method A; $t_R = 4.04$ min).

3-[[(Thienyl)carbonyl]-amino]-4-methyl-*N*-(2-chloro-6-methylphenyl)-1,3-thiazole-5-carboxamide (7i): ^{1}H NMR (400 MHz, DMSO-d_6) δ 12.74 (s, 1H), 9.62 (s, 1H), 8.63 (s, 1H), 7.75 (dd, $J = 5.09$, 1.02 Hz, 1H), 7.68−7.71 (m, 1H), 7.34−7.41 (m, 1H), 7.22−7.30 (m, 2H), 2.59 (s, 3H), 2.24 (s, 3H). HRMS (ESI) *m*/*z* calcd for $C_{17}H_{15}ClN_3O_2S_2$ $[M + H]^+$, 392.0294; found, 392.0288. Purity: 97% (method A; $t_R = 3.71$ min).

2-[[(Thienyl)carbonyl]-amino]-4-methyl-*N*-(2-chloro-6-methylphenyl)-1,3-thiazole-5-carboxamide (7j): ^{1}H NMR (400 MHz, DMSO-d_6) δ 12.91 (s, 1H), 9.63 (s, 1H), 8.24 (s, 1H), 7.98 (d, $J = 4.58$ Hz, 1H), 7.38 (dd, $J = 7.38$, 1.78 Hz, 1H), 7.17−7.32 (m, 3H), 2.58 (s, 3H), 2.24 (s, 3H). HRMS (ESI) *m*/*z* calcd for $C_{17}H_{15}ClN_3O_2S_2$ $[M + H]^+$, 392.0294; found, 392.0293. Purity: 96% (method A; $t_R = 3.7$ min).

2-[[(Furanyl)carbonyl]-amino]-4-methyl-*N*-(2-chloro-6-methylphenyl)-1,3-thiazole-5-carboxamide (7k): ^{1}H NMR (400 MHz, DMSO-d_6) δ 12.80 (s, 1H), 9.64 (s, 1H), 8.03 (s, 1H), 7.70 (s, 1H), 7.38 (dd, $J = 7.12$, 2.03 Hz, 1H), 7.19−7.31 (m, 2H), 6.70−6.79 (m, 1H), 2.58 (s, 3H), 2.23 (s, 3H). HRMS (ESI) *m*/*z* calcd for $C_{17}H_{15}ClN_3O_3S$ $[M + H]^+$, 376.0522; found, 376.0532. Purity: 98% (method A; $t_R = 3.49$ min).

2-[(Benzoyl)-amino]-4-methyl-*N*-(2-chloro-6-methylphenyl)-1,3-thiazole-5-carboxamide (7l): ^{1}H NMR (400 MHz, DMSO-d_6) δ 12.92 (s, 1H), 9.65 (s, 1H), 8.11 (d, $J = 7.63$ Hz, 2H), 7.64 (d, $J = 7.63$ Hz, 1H), 7.55 (t, $J = 7.63$ Hz, 2H), 7.36−7.41 (m, 1H), 7.21−7.30 (m, 2H), 2.59 (s, 3H), 2.24 (s, 3H). HRMS (ESI) *m*/*z* calcd for $C_{19}H_{17}ClN_3O_2S$ $[M + H]^+$, 386.0730; found, 386.0739. Purity: >95% (method A; $t_R = 3.79$ min).

2-[[(Cyclopropyl)carbonyl]-amino]-4-methyl-*N*-(2-chloro-6-methylphenyl)-1,3-thiazole-5-carboxamide (7m): ^{1}H NMR (400 MHz, DMSO-d_6) δ 12.63 (s, 1H), 9.54 (s, 1H), 7.37 (dd, J=7.12, 2.03 Hz, 1H), 7.19−7.30 (m, 2H), 2.53 (s, 3H), 2.21 (s, 3H), 1.90−1.98 (m, 1H), 0.88−0.96 (m, 4H). HRMS (ESI) *m*/*z* calcd for $C_{16}H_{17}ClN_3O_2S$ $[M + H]^+$, 350.0730; found, 350.0741. Purity: 95% (method A; $t_R = 3.41$ min).

2-Acetamido-4-methyl-*N*-(2,4,6-trimethylphenyl)-1,3-thiazole-5-carboxamide (7c): A solution of **1** (54 mg, 0.2 mmol), acetic anhydride (22 μL, 0.23 mmol) and 4-(N,N-dimethylamino)pyridine (3 mg) in CH_2Cl_2 (4.5 mL) was stirred at rt for 4.5 h. The mixture was diluted with CH_2Cl_2 and washed with 1 N aq HCl solution and water, dried ($MgSO_4$), filtered, and concentrated. The residue was chromatographed on a silical gel column. Elution with 35% EtOAc in hexanes afforded **7c** (43 mg, 69%) as a white solid. ^{1}H NMR (400 MHz, DMSO-d_6) δ 12.34 (s, 1H), 9.24 (s, 1H), 6.91 (s, 2H), 2.53 (s, 3H), 2.25 (s, 3H), 2.17 (s, 3H), 2.13 (s, 6H). HRMS (ESI) *m*/*z* calcd for $C_{16}H_{20}N_3O_2S$ $[M + H]^+$, 318.1276; found, 318.1276. Purity: 98% (method D; $t_R = 2.7$ min), Purity: 95% (method E; $t_R = 25.07$ min).

2-[[(Phenylamino)-carbonyl]amino]-4-methyl-*N*-(2,4,6-trimethylphenyl)-1,3-thiazole-5-carboxamide (8b): A solution of **1** (80 mg, 0.29 mmol) and phenyl isocyanate (103.5 mg, 0.87 mmol) in THF (3.5 mL) and pyridine (2 mL) was heated to 60−70 °C for 5 h. The mixture was cooled to room temperature, diluted with CH_2Cl_2, washed with 1 N aq HCl solution, water, and brine, dried ($MgSO_4$), filtered, and concentrated. The residue was purified by chromatography on a silica gel column. Elution with 20% EtOAc in hexanes followed by 40% EtOAc in hexane afforded **8b** (60 mg, 52%) as a white solid. ^{1}H NMR (270 MHz, $CDCl_3$ + CD_3OD) δ 7.5 (d, 2H), 7.35 (t, 2H), 7.15 (t, 1H), 6.95 (s, 2H), 2.65 (s, 3H), 2.3 (s, 3H), 2.25 (s, 6H). HRMS (ESI) *m*/*z* calcd for

$C_{21}H_{23}N_4O_2S$ [M + H]$^+$, 395.1541; found, 395.1533. Purity: >95% (method B; t_R = 30.45 min).

2-[[(Methylamino)-carbonyl]amino]-4-methyl-*N*-(2,4,6-trimethylphenyl)-1,3-thiazole-5-carboxamide (8a): ^{1}H NMR (270 MHz, CD_3OD) δ 6.95 (s, 2H), 2.9 (s, 3H), 2.65 (s, 3H), 2.3 (s, 3H), 2.2 (s, 6H). HRMS (ESI) *m*/*z* calcd for $C_{16}H_{21}N_4O_2S$ [M + H]$^+$, 333.1385; found, 333.1373. Purity: >95% (method B; t_R = 24.48 min).

2-[[(Butylamino)-carbonyl]amino]-4-methyl-*N*-(2,4,6-trimethylphenyl)-1,3-thiazole-5-carboxamide (8c): ^{1}H NMR (270 MHz, $CDCl_3$ + CD_3OD) 6.92 (s, 2H), 3.28 (t, *J* = 7 Hz, 2H), 2.63 (s, 3H), 2.28 (s, 3H), 2.22 (s, 6H), 1.54 (m, 2H), 1.39 (m, 2H), 0.95 (t, *J* = 7 Hz, 3H). HRMS (ESI) *m*/*z* calcd for $C_{19}H_{27}N_4O_2S$ [M + H]$^+$, 375.1854; found, 375.1845. Purity: >95% (method B; t_R = 30.49 min).

2-[[(*tert*-Butylamino)carbonyl]-amino]-4-methyl-*N*-(2,4,6-trimethylphenyl)-1,3-thiazole-5-carboxamide (8d): Phenyl chloroformate (1.39 mL, 11.1 mmol) was added dropwise to a stirred biphasic solution of **1** (1.02 g, 3.7 mmol) and 10% aq $KHCO_3$ solution (170 mL) in THF (130 mL). The mixture was stirred at rt overnight, diluted with CH_2Cl_2 (200 mL), and washed with water and brine. The organic extract was separated, dried ($MgSO_4$), filtered, and concentrated. The residue was chromatographed on a silica gel column. Elution with 10% EtOAc in hexanes afforded phenyl carbamate (980 mg, 69%). ^{1}H NMR (270 MHz, DMSO-d_6) δ 12.55 (br s, 1H), 9.25 (s, 1H), 7.45 (m, 2H), 7.3 (m, 3H), 6.9 (s, 2H), 2.52 (s, 3H), 2.2 (s, 3H), 2.1 (s, 6H). MS (ESI) *m*/*z* 408 [M + H]$^+$.

A solution of phenyl carbamate (20 mg, 0.054 mmol) and *tert*-butyl amine (6 mg, 0.08 mmol) in THF-CH_3CN (3 mL, 1:1) was heated to 60 °C overnight. The solution was cooled to rt, diluted with CH_2Cl_2, washed with 1 N aq. HCl solution, and 1 N aq. NaOH solution. The organic extract was dried ($MgSO_4$), filtered, and concentrated to obtain **8d** (16 mg, 84%) as a white solid. ^{1}H NMR (400 MHz, DMSO-d_6) δ 10.20 (s, 1H), 9.04 (s, 1H), 6.88 (s, 2H), 6.54 (s, 1H), 2.44 (s, 3H), 2.23 (s, 3H), 2.11 (s, 6H), 1.30 (s, 9H). HRMS (ESI) *m*/*z* calcd for $C_{19}H_{27}N_4O_2S$ [M + H]$^+$, 375.1855; found, 375.1838. Purity: 99% (method B, 8 min gradient; t_R = 8.48 min).

2-[[(Benzylamino)carbonyl]-amino]-4-methyl-*N*-(2,4,6-trimethylphenyl)-1,3-thiazole-5-carboxamide (8e): ^{1}H NMR (400 MHz, DMSO-d_6) δ 10.73 (s, 1H), 9.07 (s, 1H), 7.34 (t, 2H), 7.29 (t, 2H), 7.25 (t, *J* = 6.87 Hz, 1H), 7.09 (br s, 1H), 6.88 (s, 2H), 4.34 (d, *J* = 6.10 Hz, 2H), 2.46 (s, 3H), 2.22 (s, 3H), 2.11 (s, 6H). HRMS (ESI) *m*/*z* calcd for $C_{22}H_{25}N_4O_2S$ [M + H]$^+$, 409.1698; found, 409.1683. Purity: 100% (method E, 8 min gradient; t_R = 8.52 min).

2-[[(*n*-Butylamino)carbonyl]-amino]-4-methyl-*N*-(2-chloro-6-methylphenyl)-1,3-thiazole-5-carboxamide (8f): ^{1}H NMR (400 MHz, CD_3OD) δ 7.48 (dd, *J* = 6.9, 3.7 Hz, 1H), 7.35 (m, 2H), 3.4 (t, *J* = 7 Hz, 2H), 2.7 (s, 3H), 2.46 (s, 3H), 1.66 (m, 2H), 1.55 (m, 2H), 1.12 (t, *J* = 7 Hz, 3H). MS (ESI) *m*/*z* 381.1 [M + H]$^+$. Purity: 100% (method F; t_R = 4.51 min).

***N*-(2-Chloro-6-methylphenyl)-2-[(cyclopropylcarbonyl)amino]-1,3-thiazole-5-carboxamide (7n):** 2-*tert*-Butoxycarbonyloxyamino-thiazole-5-carboxylic acid **4c** was prepared from ethyl 2-aminothiazole-5-carboxylate **3b** following the procedure used in the preparation of **4a**. A 2 M solution of oxalyl chloride (1 mL, 2 mmol) was added dropwise to a stirred solution of 2-*tert*-butoxycarbonyloxyamino-thiazole-5-carboxylic acid **4c** (234 mg, 1 mmol) and DMF (3 drops) in THF (10 mL). The solution was stirred at rt for 4 h and concentrated under reduced pressure and in vacuo to obtain the crude acid chloride of **4c**.

2-Chloro-6-methylaniline (212 mg, 1.5 mmol) was added dropwise to a stirred solution of crude acid chloride (~1 mmol) in CH_2Cl_2 (10 mL) at 0 °C. Diisopropylethylamine (516 mg, 4 mmol) was added. The solution was warmed to rt and stirred for 24 h, diluted with CH_2Cl_2 (60 mL), and washed with 2 N aq HCl solution (15 mL). The organic extract was separated, dried ($MgSO_4$), filtered, and concentrated. The residue was diluted with EtOAc−Et_2O (25 mL, 4:1). The solid was filtered, washed with ether, and dried in vacuo to obtain **5k** (R = 2-Cl, 6-Me) as a tan solid (175 mg, 48%).

A solution of **5k** (175 mg, 0.48 mmol) in trifluoroacetic acid (1 mL) and CH_2Cl_2 (1 mL) was stirred at 0 °C for 2 h and concentrated in vacuo. The residue was diluted with CH_2Cl_2, washed with water, satd $NaHCO_3$ solution, dried (Na_2SO_4), and concentrated to obtain **6b** (R = 2-Cl,6-Me) as a glassy solid (51 mg, 40%). ^{1}H NMR (400 MHz, DMSO-d_6) δ 9.62 (s, 1H), 7.85 (s, 1H), 7.60 (s, 2H), 7.36 (dd, *J* = 7.38, 1.78 Hz, 1H), 7.16−7.29 (m, 2H), 2.19 (s, 3H). ^{13}C NMR (DMSO-d_6) δ 18.2, 120.6, 126.8, 127.9, 128.9, 132.4, 133.6, 138.8, 142.9, 159.5. MS (ESI) 268.23 [M + H]$^+$.

A solution of amine **6b** [R = 2-Cl,6-Me] (51 mg, 0.19 mmol) and cyclopropanecarboxylic acid anhydride (302 mg, 1.96 mmol) in dioxane (2 mL) was heated to 93 °C overnight. The mixture was cooled to rt and concentrated in vacuo. The residue was diluted with EtOAc, washed with satd $KHCO_3$ solution, dried (Na_2SO_4), filtered, and concentrated. The residue was triturated with ether to obtain **7n** (11 mg, 18%) as a white solid. ^{1}H NMR (400 MHz, DMSO-d_6) δ 12.71 (br s, 1H), 10.02 (s, 1H), 8.28 (s, 1H), 7.39 (dd, *J* = 7.38, 1.78 Hz, 1H), 7.23−7.31 (m, 2H), 2.21 (s, 3H), 1.97 (ddd, *J* = 12.08, 7.25, 5.09 Hz, 1H), 0.89−0.98 (m, 4H). HRMS (ESI) *m*/*z* calcd for $C_{15}H_{15}ClN_3O_2S$ [M + H]$^+$, 336.0573; found, 336.0569. Purity: 100% (method D; t_R = 2.52 min), 100% (method F; t_R = 3.25 min).

***N*-(2-Chloro-6-methylphenyl)-2-[(ethylcarbonyl)amino]-1,3-thiazole-5-carboxamide (7o):** ^{1}H NMR (400 MHz, DMSO-d_6) δ 12.39 (s, 1H), 10.03 (s, 1H), 8.27 (s, 1H), 7.39 (d, *J* = 7.4 Hz, 1H), 7.21−7.34 (m, 2H), 3.37 (q, *J* = 7.5 Hz, 2H), 2.22 (s, 3H), 1.11 (t, *J* = 7.6 Hz, 3H). HRMS (ESI) *m*/*z* calcd for $C_{14}H_{15}ClN_3O_2S$ [M + H]$^+$, 324.0573; found, 324.0580. Purity: 95% (method A; t_R = 3.53 min), 96% (method D; t_R = 2.39 min).

***N*-(2-Chloro-6-methylphenyl)-2-[(phenylcarbonyl)amino]-1,3-thiazole-5-carboxamide (7r):** ^{1}H NMR (400 MHz, DMSO-d_6) δ 12.99 (s, 1H), 10.09 (s, 1H), 8.38 (s, 1H), 8.12 (d, *J* = 7.63 Hz, 2H), 7.66 (t, *J* = 7.38 Hz, 1H), 7.52−7.62 (m, 2H), 7.41 (dd, *J* = 7.63, 2.03 Hz, 1H), 7.23−7.33 (m, 2H), 2.24 (s, 3H). HRMS (ESI) *m*/*z* calcd for $C_{18}H_{15}ClN_3O_2S$ [M + H]$^+$, 372.0573; found, 372.0569. Purity: 94% (method A; t_R = 3.61 min), >95% (method D; t_R = 2.94 min).

***N*-(2-Chloro-6-methylphenyl)-2-[(2-thienylcarbonyl)amino]-1,3-thiazole-5-carboxamide (7s):** ^{1}H NMR (400 MHz, DMSO-d_6) δ 13.09 (s, 1H), 10.10 (s, 1H), 8.39 (s, 1H), 8.32 (s, 1H), 8.03 (d, *J* = 4.07 Hz, 1H), 7.42 (dd, *J* = 7.63, 2.03 Hz, 1H), 7.20−7.36 (m, 3H), 2.25 (s, 3H). HRMS (ESI) *m*/*z* calcd for $C_{16}H_{13}ClN_3O_2S_2$ [M + H]$^+$, 378.0138; found, 378.0137. Purity: 98% (method A; t_R = 3.61 min), 93% (method D; t_R = 2.85 min).

***N*-(2-Chloro-6-methylphenyl)-2-[(3-thienylcarbonyl)amino]-1,3-thiazole-5-carboxamide (7t):** ^{1}H NMR (400 MHz, DMSO-d_6) δ 12.86 (s, 1H), 10.08 (s, 1H), 8.67 (s, 1H), 8.37 (s, 1H), 7.76 (d, *J* = 4.58 Hz, 1H), 7.71 (dd, *J* = 4.58, 2.80 Hz, 1H), 7.40 (dd, *J* = 7.38, 1.78 Hz, 1H), 7.22−7.34 (m, 2H), 2.23 (s, 3H). HRMS (ESI) *m*/*z* calcd for $C_{16}H_{13}ClN_3O_2S_2$ [M + H]$^+$, 378.0138; found, 378.0136. Purity: 98% (method A; t_R = 3.60 min), >95% (method D; t_R = 2.85 min).

***N*-(2-Chloro-6-methylphenyl)-2-[(2-furanylcarbonyl)amino]-1,3-thiazole-5-carboxamide (7u):** ^{1}H NMR (400 MHz, DMSO-d_6) δ 12.96 (s, 1H), 10.08 (s, 1H), 8.35 (s, 1H), 8.05 (s, 1H), 7.72 (s, 1H), 7.40 (dd, *J* = 7.38, 1.78 Hz, 1H), 7.19−7.33 (m, 2H), 6.76 (s, 1H), 2.23 (s, 3H). HRMS (ESI) *m*/*z* calcd for $C_{16}H_{13}ClN_3O_3S$ [M + H]$^+$, 362.0366; found, 362.0362. Purity: 95% (method A; t_R = 3.61 min), 93% (method D; t_R = 2.62 min).

***N*-(2-Chloro-6-methylphenyl)-2-[(cyclobutylcarbonyl)amino]-1,3-thiazole-5-carboxamide (7v):** ^{1}H NMR (400 MHz, DMSO-d_6) δ 12.30 (s, 1H), 10.02 (s, 1H), 8.27 (s, 1H), 7.39 (dd, *J* = 7.12, 2.03 Hz, 1H), 7.22−7.31 (m, 2H), 3.38 (m, 1H), 2.19−2.28 (m, 2H), 2.22 (s, 3H), 2.10−2.19 (m, 2H), 1.89−2.04 (m, 1H), 1.78−1.87 (m, 1H). HRMS (ESI) *m*/*z* calcd for $C_{16}H_{17}ClN_3O_2S$ [M + H]$^+$, 350.0730; found, 350.0720. Purity: 91% (method A; t_R = 3.52 min), 90% (method D; t_R = 2.75 min).

***N*-(2-Chloro-6-methylphenyl)-2-[(cyclopentylcarbonyl)amino]-1,3-thiazole-5-carboxamide (7w):** ^{1}H NMR (400 MHz, DMSO-

d_6) δ 12.42 (s, 1H), 10.02 (s, 1H), 8.27 (s, 1H), 7.39 (dd, J = 7.38, 1.78 Hz, 1H), 7.20−7.32 (m, 2H), 2.86−3.02 (m, 1H), 2.21 (s, 3H), 1.50−1.99 (m, 8H). HRMS (ESI) m/z calcd for $C_{17}H_{19}ClN_3O_2S$ $[M + H]^+$, 364.0886; found, 364.0891. Purity: 93% (method A; t_R = 3.59 min), >95% (method D; t_R = 2.95 min).

***N*-(2-Chloro-6-methylphenyl)-2-[(2,6-dimethyl-4-pyrimidinyl)-amino]-1,3-thiazole-5-carboxamide (12m):** A solution of copper-(II) bromide (2.68 g, 12 mmol) in CH_3CN (50 mL) was purged with nitrogen and cooled to 0 °C. *t*-Butyl nitrite (2 mL, 15 mmol) was added. A solution of amine **6b** [R = 2-Cl,6-Me] (2.68 g, 10 mmol) in AcCN (50 mL) was added. The mixture was stirred at rt and concentrated, and the residue was dissolved in EtOAc and washed with satd $NaHCO_3$ solution. The precipitate was removed by filtration, and the EtOAc extract was dried (Na_2SO_4), filtered, and concentrated. The residue was crystallized from EtOAc/ether/hexanes mixture to obtain bromide **11** [R = 2-Cl,6-Me] (1.68 g, 51%) as a yellow solid. ^{1}H NMR (500 MHz, DMSO-d_6) δ 10.39 (s, 1H), 8.44 (s, 1H), 7.41 (dd, J = 7.15, 2.20 Hz, 1H), 7.24−7.32 (m, 2H), 2.22 (s, 3H). HRMS (ESI) m/z calcd for $C_{11}H_8N_2OSBrCl$ $[M - H]^-$, 328.9150; found, 328.9153.

Sodium hydride (95%; 609 mg, 24.1 mmol) was added to a solution of bromide **11** [R = 2-Cl,6-Me] (1 g, 3.02 mmol) and 2,6-dimethyl-4-amino-pyrimidine (1.49 g, 12.06 mmol) in THF (10 mL). The solution was heated under reflux overnight, cooled to rt, and quenched by addition of glacial acetic acid and methanol. The reaction mixture was concentrated, and the residue was diluted with water and saturated aq $NaHCO_3$ solution. The solid was collected by filtration, washed with water and a minimal amount of methanol, and dried in vacuo to obtain a pale yellow solid that was suspended in MeOH and treated with concd HCl (62 μL, 0.74 mmol). The solution was concentrated and triturated with EtOH and ether to obtain **12m** as its hydrochloride salt (240 mg, 19%) as a light yellow solid. ^{1}H NMR (400 MHz, DMSO-d_6) δ 11.96 (s, 1H), 9.96 (s, 1H), 8.29 (s, 1H), 7.41 (m, 1H), 7.28 (m, 2H), 6.74 (s, 1H), 2.56 (s, 3H), 2.36 (s, 3H), 2.25 (s, 3H). HRMS (ESI) m/z calcd for $C_{17}H_{17}ClN_5OS$ $[M + H]^+$, 374.0842; found, 374.0840. Purity: 100% (method A; t_R = 2.64 min), >95% (method D; t_R = 2.07 min).

***N*-(2-Chloro-6-methylphenyl)-2-[(3-pyridinyl)amino]-1,3-thiazole-5-carboxamide (12b):** ^{1}H NMR (500 MHz, DMSO-d_6) δ 10.81 (s, 1H), 9.95 (s, 1H), 8.77 (d, J = 2.20 Hz, 1H), 8.16−8.24 (m, 2H), 8.15 (s, 1H), 7.34−7.42 (m, 2H), 7.21−7.31 (m, 2H), 2.23 (s, 3H). HRMS (ESI) m/z calcd for $C_{16}H_{14}ClN_4OS$ $[M + H]^+$, 345.0578; found, 345.0576. Purity: 99% (method A; t_R = 2.47 min).

***N*-(2-Chloro-6-methylphenyl)-2-[(4-pyridinyl)amino]-1,3-thiazole-5-carboxamide (12c):** ^{1}H NMR (500 MHz, DMSO-d_6) δ 11.70 (s, 1H), 10.13 (s, 1H), 8.53 (d, J = 6.60 Hz, 2H), 8.29 (s, 1H), 7.86 (d, J = 3.85 Hz, 2H), 7.40 (d, J = 7.70 Hz, 1H), 7.23−7.32 (m, 2H), 2.23 (s, 3H). HRMS (ESI) m/z calcd for $C_{16}H_{14}ClN_4OS$ $[M + H]^+$, 345.0578; found, 345.0564. Purity: 97% (method A; t_R = 2.49 min).

***N*-(2,4,6-Trimethylphenyl)-2-[(2-pyridinyl)amino]-1,3-thiazole-5-carboxamide (12e):** ^{1}H NMR (500 MHz, DMSO-d_6) δ 11.61 (s, 1H), 9.50 (s, 1H), 8.35 (d, J = 3.85 Hz, 1H), 8.19 (s, 1H), 7.71−7.78 (m, 1H), 7.10 (d, J = 8.25 Hz, 1H), 6.98 (dd, J = 6.87, 5.22 Hz, 1H), 6.91 (s, 2H), 2.24 (s, 3H), 2.13 (s, 6H). HRMS (ESI) m/z calcd for $C_{18}H_{19}N_4OS$ $[M + H]^+$, 339.1280; found, 339.1272. Purity: 99% (method A; t_R = 3.66 min).

***N*-(2,6-Dimethylphenyl)-2-[(3-pyradizinyl)amino]-1,3-thiazole-5-carboxamide (12g):** ^{1}H NMR (500 MHz, DMSO-d_6) δ 11.85 (s, 1H), 9.67 (s, 1H), 8.88 (d, J = 4.4 Hz, 1H), 8.25 (s, 1H), 7.64 (dd, J = 8.8, 4.4 Hz, 1H), 7.41 (d, J = 8.8 Hz, 1H), 7.11 (s, 3H), 2.19 (s, 6H). HRMS (ESI) m/z calcd for $C_{16}H_{16}N_5OS$ $[M + H]^+$, 326.1070; found, 326.1076. Purity: 95% (method A; t_R = 2.97 min).

***N*-(2-Chloro-6-methylphenyl)-2-[(3,5-dimethyl-2-pyrazinyl)-amino]-1,3-thiazole-5-carboxamide (12h):** ^{1}H NMR (500 MHz, DMSO-d_6) δ 11.17 (s, 1H), 9.89 (s, 1H), 8.29 (s, 1H), 8.12 (s, 1H), 7.38 (d, J = 7.7 Hz, 1H), 7.21−7.31 (m, 2H), 2.57 (s, 3H), 2.39 (s, 3H), 2.23 (s, 3H). HRMS (ESI) m/z calcd for $C_{17}H_{17}ClN_5OS$ $[M + H]^+$, 374.0843; found, 374.0854. Purity: 99% (method A; t_R = 3.58 min).

***N*-(2-Chloro-6-methylphenyl)-2-[(6-methyl-2-pyridinyl)amino]-1,3-thiazole-5-carboxamide (12j):** ^{1}H NMR (500 MHz, DMSO-d_6) δ 11.59 (s, 1H), 9.83 (s, 1H), 8.24 (s, 1H), 7.63 (t, J = 7.79 Hz, 1H), 7.39 (d, J = 7.33 Hz, 1H), 7.21−7.31 (m, 2H), 6.90 (d, J = 8.25 Hz, 1H), 6.85 (d, J = 7.79 Hz, 1H), 2.50 (s, 3H), 2.24 (s, 3H). HRMS (ESI) m/z calcd for $C_{17}H_{16}ClN_4OS$ $[M + H]^+$, 359.0734; found, 359.0731. Purity: >95% (method A; t_R = 3.61 min).

***N*-(2-Chloro-6-methylphenyl)-2-[(4-methyl-2-pyridinyl)amino]-1,3-thiazole-5-carboxamide (12k):** ^{1}H NMR (500 MHz, DMSO-d_6) δ 11.59 (s, 1H), 9.83 (s, 1H), 8.17−8.25 (m, 2H), 7.38 (dd, J = 7.7, 1.65 Hz, 1H), 7.21−7.30 (m, 2H), 6.91 (s, 1H), 6.84 (d, J = 5.5 Hz, 1H), 2.30 (s, 3H), 2.23 (s, 3H). HRMS (ESI) m/z calcd for $C_{17}H_{16}ClN_4OS$ $[M + H]^+$, 359.0734; found, 359.0741. Purity: 98% (method A; t_R = 3.29 min).

***N*-(2-Chloro-6-methylphenyl)-2-[(4,6-dimethyl-2-pyridinyl)-amino]-1,3-thiazole-5-carboxamide (12l):** ^{1}H NMR (400 MHz, DMSO-d_6) δ 11.53 (s, 1H), 9.82 (s, 1H), 8.23 (s, 1H), 7.39 (d, J = 7.63 Hz, 1H), 7.16−7.34 (m, 2H), 6.70 (d, J = 2.54 Hz, 2H), 2.43 (s, 3H), 2.25 (s, 3H), 2.23 (s, 3H). MS (ESI) m/z 373 $[M + H]^+$. Purity: >98% (method A; t_R = 3.58 min).

2-Chloro-*N*-[2-chloro-6-methylphenyl]-1,3-thiazole-5-carboxamide (14): A 2.5 M solution of *n*-butyllithium in hexanes (1.68 mL, 4.2 mmol) was added dropwise to a solution of 2-chlorothiazole **13** (480 mg, 4 mmol) in THF (10 mL) at −78 °C. The reaction mixture was maintained below −75 °C during addition. After 15 min, a solution of 2-chloro-6-methylphenyl isocyanate (600 μL, 4.4 mmol) in THF (5 mL) was added. The solution was stirred at −78 °C for 2 h, quenched by addition of saturated aq NH_4Cl solution (10 mL), and partitioned between EtOAc and water. The EtOAc extract was separated, washed with brine, dried ($MgSO_4$), filtered, and concentrated. The residue was crystallized from EtOAc−hexanes to obtain **14** (988 mg, 86%) as a pale yellow solid. ^{1}H NMR (400 MHz, $CDCl_3$) δ 8.08 (s, 1H), 7.97 (s, 1H), 7.27 (m, 1H), 7.16 (m, 2H), 2.25 (s, 3H). MS (ESI) m/z 286 $[M + H]^+$.

***N*-(4-Methoxybenzyl)-2-chloro-[2-chloro-6-methylphenyl]-1,3-thiazole-5-carboxamide (15):** Sodium hydride (95% dispersion, 60 mg, 2.4 mmol) was added to a solution of **14** (574 mg, 2 mmol) in DMF (5 mL). After 30 min, the mixture was treated with 4-methoxybenzyl chloride (325 μL, 2.4 mmol) and tetrabutylammonium iodide (148 mg, 0.4 mmol) and then stirred at rt for 16 h. The mixture was diluted with EtOAc and water. The EtOAc extract was separated, washed with brine, dried ($MgSO_4$), filtered, and concentrated. The residue was chromatographed on a silica gel column and eluted with 90% EtOAc in hexanes to obtain **15** as a colorless viscous oil (95% dispersion, 676 mg, 95%). ^{1}H NMR (400 MHz, DMSO-d_6) δ 7.48 (d, J = 8.3 Hz, 1H), 7.42 (s, 1H), 7.41 (dd, J = 7.7, 8.3 Hz, 1H), 7.28 (d, J = 7.7 Hz, 1H), 7.11 (d, J = 8.3 Hz, 2H), 6.78 (d, J = 8.8 Hz, 2H), 5.85 (d, J = 14.0 Hz, 1H), 4.50 (d, J = 14.0 Hz, 1H), 3.66 (s, 3H), 1.72 (s, 3H). ^{13}C NMR (100 MHz, DMSO-d_6) δ 159.3, 155.3, 145.8, 140.5,136.1, 134.0, 133.7, 131.6, 131.5, 130.9, 128.9, 127.6, 113.9, 55.2, 51.6, 17.9. MS (ESI) m/z 408 $(M + H)^+$.

***N*-(4-Methoxybenzyl)-2-(6-chloro-2-methylpyrimidin-4-ylamino)-*N*-(2-chloro-6-methylphenyl)-1,3-thiazole-5-carboxamide (16):** 4-Amino-6-chloro-2-methylpyrimidine (14.4 g, 0.10 mol) was added in portions to a suspension of sodium hydride (60% dispersion, 12.0 g, 0.30 mol) in THF (300 mL) at 0 °C. After 30 min, **15** (27.2 g, 0.067 mol) was added in portions. The mixture was heated at reflux for 4 h, cooled to room temperature, and diluted with H_2O (10 mL). The mixture was acidified with 1 N HCl (500 mL) and extracted with 10% MeOH in chloroform (250 mL, 3×). The combined extracts were dried ($MgSO_4$), filtered, and concentrated in vacuo to obtain a solid that was triturated with ether to give **16** (28.4 g, 83%). ^{1}H NMR (400 MHz, DMSO-d_6) δ 7.54 (d, J = 8.5 Hz, 1H), 7.46 (s, 1H), 7.43 (dd, J = 8.3, 7.7 Hz, 1H), 7.30 (d, J = 7.7 Hz, 1H), 7.16 (d, J = 8.3 Hz, 2H), 6.74 (s, 1H), 6.83 (d, J =

8.8 Hz, 2H), 5.21 (d, J = 13.7 Hz, 1H), 4.44 (d, J = 13.7 Hz, 1H), 3.71 (s, 3H), 2.45 (s, 3H), 1.72 (s, 3H). MS (ESI) m/z 515 $(M + H)^+$.

2-(6-Chloro-2-methylpyrimidin-4-ylamino)-*N*-(2-chloro-6-methylphenyl)-1,3-thiazole-5-carboxamide (17): A solution of **16** (6.6 g, 13 mmol) dissolved in a mixture of CH_2Cl_2 and TFA (50 mL, 1:1) was treated with triflic acid (6.8 g, 45 mmol) and stirred at rt for 3 h. The mixture was poured onto crushed ice (150 g) and extracted with $CHCl_3$ (100 mL, 3×). The desired product precipitated from solution upon standing at room temperature and was collected by filtration and dried in vacuo to give compound **17** (5.0 g, 99%). ^{1}H NMR (400 MHz, DMSO-d_6) δ 12.24 (br s, 1H), 10.02 (s, 1H), 8.32 (s, 1H), 7.41 (d, J = 7.7 Hz, 1H), 7.30 (dd, J = 6.1, 6.7 Hz, 1H), 7.26 (d, J = 7.7 Hz, 1H), 6.95 (s, 1H), 2.59 (s, 3H), 2.24 (s, 3H). MS (ESI) m/z 395 $(M + H)^+$.

***N*-(2-Chloro-6-methylphenyl)-2-[[6-[4-(2-hydroxyethyl)-1-piperazinyl)]-2-methyl-4-pyrimidinyl]amino)]-1,3-thiazole-5-carboxamide, Hydrochloride Salt (2):** A mixture of **17** (34.7 g, 88.1 mmol), diisopropylethylamine (3.6 mL, 0.17 mol), and 1-(2-hydroxyethyl)piperazine (54 mL, 0.44 mol) in 1,4-dioxane (300 mL) was refluxed for 12 h. The mixture was concentrated under vacuum, and the solid was triturated successively with H_2O, aqueous MeOH, and Et_2O (2×) and dried in vacuo. The solid was resuspended in ether−methanol, treated with 2 N HCl (44 mL), and vigorously stirred for 30 min. The precipitate was collected by filtration and triturated successively with ether, ether−methanol, and then ether. The solid was dried in vacuo to give **2** (42.2 g, 91%) as its hydrochloride salt. Mp = 279−280 °C (free base). ^{1}H NMR (400 MHz, DMSO-d_6) δ 11.67 (br s, 1H), 10.50 (br s, 1H), 9.96 (s, 1H), 8.27 (s, 1H), 7.40 (d, J = 7.7 Hz, 1H), 7.28 (dd, J = 6.6, 6.7 Hz, 1H), 7.25 (d, J = 7.7 H, 1 Hz), 6.17 (s, 1H), 4.33 (d, J = 12.6 Hz, 2H), 3.79 (dd, J = 5.0, 5.5 Hz, 2H), 3.60 (d, J = 11.6 Hz, 2H), 3.38 (dd, J = 12.1, 12.6 Hz, 2H), 3.22 − 3.19 (m, 2H), 3.13 − 3.07 (m, 2H), 2.45 (s, 3H), 2.24 (s, 3H). ^{13}C NMR (125 MHz, DMSO-d_6) δ 165.7, 162.8, 162.1, 160.4, 157.5, 141.2, 139.4, 133.8, 133.0, 129.6, 128.8, 127.6, 126.5, 84.0, 58.1, 55.2, 51.1 (2), 41.2 (2), 25.7, 18.8. HRMS (ESI) m/z calcd for $C_{22}H_{27}ClN_7O_2S$ $(M + H)^+$, 488.1635; found, 488.1636. Anal. Calcd for $C_{22}H_{26}ClN_7O_2S$: C, 54.14; H, 5.37; N, 20.09. Found: C, 53.90; H, 5.30; N, 20.07. Purity: 100% (method A; t_R = 2.72 min).

***N*-(2-Chloro-6-methylphenyl)-2-(6-(2-hydroxyethylamino)pyridin-2-ylamino)-1,3-thiazole-5-carboxamide (12p):** ^{1}H NMR (400 MHz, DMSO-d_6) δ 11.27 (s, 1H), 9.77 (s, 1H), 8.19 (s, 1H), 7.38 (dd, J = 2.17, 7.23 Hz, 1H), 7.32−7.22 (m, 3H), 6.16 (d, J = 7.63 Hz, 1H), 6.09 (d, J = 8.13 Hz, 1H), 3.60−3.57 (m, 2H), 3.50−3.45 (m, 2H), 2.23 (s, 3H). HRMS (ESI) m/z calcd for $C_{18}H_{19}ClN_5O_2S$ $(M + H)^+$, 404.0948; found, 404.0964. Anal. Calcd for $C_{18}H_{18}ClN_5O_2S\cdot1.0HCl\cdot0.2H_2O$: C, 48.69; H, 4.40; N, 15.77. Found: C, 48.65; H, 4.18; N, 15.59. Purity: >99% (method A; t_R = 3.08 min).

***N*-(2-Chloro-6-methylphenyl)-2-(6-(3-morpholinopropylamino)pyridin-2-ylamino)-1,3-thiazole-5-carboxamide (12q):** ^{1}H NMR (400 MHz, DMSO-d_6) δ 11.39 (s, 1H), 9.55 (s, 1H), 9.57 (br s, 1H), 8.27 (s, 1H), 7.39 (d, J = 7.63 Hz, 1H), 7.33 (dd, J = 7.63 Hz, 7.63 Hz, 1H), 7.29−7.22 (m, 2H), 6.97 (br s, 1H), 6.19 (d, J = 7.63 Hz, 1H), 6.05 (d, J = 8.13 Hz, 1H), 3.88 (d, J = 13.74 Hz, 3H), 3.55 (t, J = 11.69 Hz, 2H), 3.46−3.37 (m, 3H), 3.29−3.23 (m, 2H), 3.03−2.93 (m, 2H), 2.23 (s, 3H), 2.03−1.97 (m, 2H). HRMS (ESI) m/z calcd for $C_{23}H_{28}ClN_6O_2S$ $(M + H)^+$, 487.1683; found, 487.1696. Purity: >98% (method A; t_R = 2.87 min).

2-(6-(3-(1*H*-Imidazol-1-yl)propylamino)pyridin-2-ylamino)-*N*-(2-chloro-6-methylphenyl)-1,3-thiazole-5-carboxamide (12r): ^{1}H NMR (500 MHz, CD_3OD) δ 8.99 (s, 1H), 8.36 (s, 1H), 7.70 (s, 1H), 7.65 (br s, 1H), 7.54 (s, 1H),7.36−7.38 (dd, J = 2.2, 7.2 Hz, 1H), 7.25−7.28 (m, 2H), 6.39−6.44 (m, 2H), 4.46 (t, J = 7.4 Hz, 2H), 3.55 (t, J = 7.2 Hz, 2H), 2.32−2.36 (m, 5H). HRMS (ESI) m/z calcd for $C_{22}H_{23}ClN_7OS$ $(M + H)^+$, 468.1373; found, 468.1394. Purity: >98% (method A; t_R = 2.83 min).

***N*-(2-Chloro-6-methylphenyl)-2-(6-morpholinopyrimidin-4-ylamino)-1,3-thiazole-5-carboxamide (12s):** ^{1}H NMR (500 MHz, DMSO-d_6) δ 11.75 (br s, 1H), 9.98 (s, 1H), 8.45 (s, 1H), 8.26 (s, 1H), 7.39 (dd, J = 1.65, 7.38 Hz, 1H), 7.29−7.24 (m, 2H), 6.29 (s, 1H), 3.70−3.68 (m, 4H), 3.53−3.51 (m, 4H), 2.23 (s, 3H). HRMS (ESI) m/z calcd for $C_{19}H_{20}ClN_6O_2S$ $(M + H)^+$, 431.1057; found, 431.1055. Anal. Calcd for $C_{19}H_{19}ClN_6O_2S\cdot1.0HCl$: C, 48.83; H, 4.31; N, 17.98. Found: C, 48.76; H, 4.21; N, 17.80. Purity: >98% (method A; t_R = 3.44 min).

***N*-(2-Chloro-6-methylphenyl)-2-(2-methyl-6-morpholinopyrimidin-4-ylamino)-1,3-thiazole-5-carboxamide (12t):** ^{1}H NMR (400 MHz, DMSO-d_6) δ 11.52 (s, 1H), 9.88 (s, 1H), 8.21 (s, 1H), 7.39 (d, J = 6.10 Hz, 1H), 7.29−7.23 (m, 3H), 6.04 (s, 1H), 3.67−3.65 (m, 4H), 3.49−3.46 (m, 4H), 2.41 (s, 3H), 2.23 (s, 3H). HRMS (ESI) m/z calcd for $C_{20}H_{22}ClN_6O_2S$ $(M + H)^+$, 445.1213; found, 445.1234. Purity: 95% (method A; t_R = 3.34 min).

***N*-(2-Chloro-6-methylphenyl)-2-(2-methyl-6-(3-morpholinopropylamino)pyrimidin-4-ylamino)-1,3-thiazole-5-carboxamide (12u):** ^{1}H NMR (500 MHz, DMSO-d_6): δ 11.16 (br s, 1H), 10.08 (s, 1H), 8.33 (s, 1H), 7.40 (dd, J = 1.65, 7.38 Hz, 1H), 7.30−7.25 (m, 3H), 6.28 (br s, 1H), 4.01−3.90 (m, 2H), 3.89−3.80 (m, 2H), 3.53−3.43 (m, 2H), 3.19−3.13 (m, 2H), 3.09−3.03 (m, 2H), 2.60−2.53 (m, 2H), 2.45 (s, 3H), 2.24 (s, 3H), 2.07−1.99 (m, 2H). HRMS (ESI) m/z calcd for $C_{23}H_{29}ClN_7O_2S$ $(M + H)^+$, 502.1792; found, 502.1787. Purity: >98% (method A; t_R = 2.25 min).

***N*-(2-Chloro-6-methylphenyl)-2-(6-(2-hydroxyethylamino)-2-methylpyrimidin-4-ylamino)-1,3-thiazole-5-carboxamide (12v):** ^{1}H NMR (400 MHz, DMSO-d_6): δ 11.27 (s, 1H), 9.77 (s, 1H), 8.19 (s, 1H), 7.38 (dd, J = 2.17, 7.23 Hz, 1H), 7.32−7.22 (m, 3H), 6.16 (d, J = 7.63 Hz, 1H), 6.09 (d, J = 8.13 Hz, 1H), 3.60−3.57 (m, 2H), 3.50−3.45 (m, 2H), 2.23 (s, 3H). HRMS (ESI) m/z calcd for $C_{18}H_{20}ClN_6O_2S$ $(M + H)^+$, 419.1057; found, 419.1047. Purity: 95% (method A; t_R = 2.68 min).

***N*-(2-Chloro-6-methylphenyl)-2-(6-(4-(hydroxymethyl)piperidin-1-yl)-2-methylpyrimidin-4-ylamino)-1,3-thiazole-5-carboxamide (12w):** ^{1}H NMR (500 MHz, CD_3OD) δ 8.22 (s, 1H), 7.35 (dd, J = 7.1, 1.6 Hz, 1H), 7.26−7.23 (m, 2H), 6.39 (br s, 1H), 3.45 (d, J = 6.0 Hz, 2H), 3.31−3.29 (m, 4H), 2.65 (s, 3H), 2.31 (s, 3H), 2.00−1.80 (m, 3H), 1.35−1.32 (m, 2H). LC/MS (ESI): m/z 473 $(M + H)^+$. Purity: 98% (method A; t_R = 3.05 min).

Lck Enzyme Assay. For the preparation of recombinant Lck, human Lck was prepared as a His-tagged fusion protein using the commercially available (Life Technologies) baculovirus vector pFastBac Hta in insect cells. A cDNA encoding human Lck isolated by PCR was inserted into the vector, and the protein was expressed using the methods described by the manufacturer. The Lck purified by nickel affinity chromatography was incubated in kinase buffer (20 mM MOPS, pH 7, 10 mM $MgCl_2$) in the presence of the test compound. The reaction was initiated by the addition of the substrates to the final concentration of 1 μM ATP, 3.3 μCi/mL [^{33}P] g-ATP, and 0.1 mg/mL acid denatured enolase and was stopped after 10 min by the addition of 10% trichloroacetic acid and 100 mM sodium pyrophosphate, followed by 2 mg/mL bovine serum albumin. The labeled enolase protein substrate was precipitated at 4 °C, harvested onto Packard Unifilter plates, and counted in a Topcount scintillation counter.

T-Cell Proliferation Assay. A 96-well plate was coated with a monoclonal antibody to CD3 (G19-4), the antibody was allowed to bind, and then the plate was washed. Normal human peripheral blood T-cells were added to the wells, along with the test compound and anti-CD28 antibody (E.3), to provide costimulation. After 3 days, the [^{3}H]-thymidine was added to the cells, further incubation occurred, and the cells were harvested and counted in a scintillation counter to measure proliferation.

Inhibition of IL-2 Production Ex Vivo in Mice. BALB/c female mice were dosed by oral gavage (po) with either vehicle alone (propylene glycol−water, 1:1, v/v) or compound **12m** dissolved in vehicle. After 2 h, blood was collected into heparain anticoagulant. Triplicate cultures of each sample containing 100 μL whole blood and anti-CD3 antibody (10 μg/mL), anti-CD28 antibody (10 μg/mL), and goat anti-hamster IgG antibody (30 μg/mL) were established in 96-well plates. Plates were incubated for 24 h at 37 °C in 5% CO_2. Culture supernatants were collected and

assayed for IL-2 concentration by ELISA. Results are shown as mean ± SEM of $n = 7$ mice per treatment group.

Inhibition of Tumor Necrosis Factor α (TNFα) in Mice. C57BL/6 female mice, 8−10 weeks of age (Harlan Teklad, Indianapolis, IN), were dosed by oral gavage (po) with either vehicle alone (propylene glycol−water, 1:1, v/v) or compound **12m** dissolved in vehicle. After 2 h, mice were injected intravenously (iv) with 500 μg/kg lipopolysaccharide (LPS, *Escherichia coli* 0111: B4; Sigma, St. Louis, MO). Mice were bled 1 h after LPS injection. Serum was separated from clotted blood samples by centrifugation (5 min, 5000 × *g*, room temperature) and analyzed for the levels of TNFα by ELISA assay according to manufacturer's instructions (R&D systems, Minneapolis, MN). Results are shown as mean ± SEM of $n = 11-12$ mice per treatment group.

Adjuvant Arthritis in Rats: Treatment of Established Disease. Male Lewis rats (150−175 g; Harlan Teklad, Indianapolis, IN) were immunized at the base of the tail with complete Freund's adjuvant. The volumes of their hind paws were measured in a water displacement plethysmometer (Ugo Basile, Italy). Fourteen days after immunization, when disease was clinically evident, rats were randomized into treatment groups ($n = 8$/group). Rats were treated orally twice daily with **12m** at 0.3 mg/kg and 3.0 mg/kg in a vehicle solution of propylene glycol/H_2O (1:1). Control rats received vehicle alone. All procedures involving animals were reviewed and approved by the Institutional Animal Care and Use Committee.

Acknowledgment. We are greatly indebted to Emily Luk and Bethanne Warrack of Bioanalytical and Discovery Analytical Sciences for analytical support and Bei Wang of the Department of Chemical Synthesis for the synthesis of an advanced intermediate.

References

(1) (a) Molina, T. J.; Kishihara, K.; Siderovski, D. P.; van Ewijk, W.; Narendran, A.; Timms, E.; Wakeham, A.; Paige, C. J.; Hartman, K.-U.; Veilette, A.; Davison, D.; Mak, T. W. Profound block in thymocyte development in mice lacking p56lck. *Nature* **1992**, *357*, 161−4. (b) Levin, S. D.; Anderson, S. J.; Forbush, K. A.; Perlmutter, R. M. A dominant-negative transgene defines a role for p56lck in thymopoiesis. *EMBO J.* **1993**, *12*, 1671−80.

(2) (a) Straus, D. B.; Weiss, A. Genetic evidence for the involvement of the lck tyrosine kinase in signal transduction through the T cell antigen receptor. *Cell* **1992**, *70*, 585−93. (b) Chan, A. C.; Desai, D. M.; Weiss, A. C. The role of protein tyrosine kinases and protein tyrosine phosphatases in T cell antigen receptor signal transduction. *Ann. Rev. Immunol.* **1994**, *12*, 555−92. (c) Weiss, A.; Littman, D. Signal transduction by lymphocyte antigen receptors. *Cell* **1994**, *76*, 263−74. (d) Hanke, J. H.; Gardner, J. P.; Dow, R. L.; Changelian, P. S.; Brissette, W. H.; Weringer, E. J.; Pollok, B. A.; Connelly, P. A. Discovery of a novel, potent, and Src-selective tyrosine kinase inhibitor. Study of Lck- and Fyn T-dependent T cell activation. *J. Biol. Chem.* **1996**, *271*, 695−701. (e) van Oers, N. S.; Lowin-Kropf, B.; Connolly, K.; Weiss, A. α/β T cell development is abolished in mice lacking both Lck and Fyn protein tyrosine kinases. *Immunity* **1996**, *5*, 429−36.

(3) Wen, T.; Zhang, L.; Kung, S. K. P.; Molina, T. J.; Miller, R. G.; Mak, T. W. Allo-skin graft rejection, tumor rejection, and natural killer activity in mice lacking p56lck. *Eur. J. Immunol.* **1995**, *25*, 3155−9.

(4) (a) Kamens, J. S.; Ratnofsky, S. E.; Hirst, G. C. Lck inhibitors as a therapeutic approach to autoimmune disease and transplant rejection. *Curr. Opin. Invest. Drugs* **2001**, *2*, 1213−19. (b) Dowden, J.; Ward, S. G. Inhibitors of $p56^{lck}$: assessing their potential as tools for manipulating T-lymphocyte activation. *Expert Opin. Ther. Pat.* **2001**, *11*, 295−306. (c) Boschelli, D. H.; Boschelli, F. Small molecule inhibitors of Src family kinases. *Drugs Future* **2000**, *25*, 717−36. (d) Susa, M.; Teti, A. Tyrosine kinase src inhibitors: potential therapeutic applications. *Drug News Perspect.* **2000**, *13*, 169−75.

(5) (a) Majolini, M. B.; Boncristiano, M; Baldari, C. T. Dysregulation of the protein tyrosine kinase LCK in lymphoproliferative disorders and in other neoplasias. *Leuk. Lymphoma* **1999**, *35*, 245−54. (b) Yu, C. L.; Jove, R.; Burakoff, S. J. Constititive activation of the Janus kinase-STAT pathway in T lymphoma overexpressing the Lck protein tyrosine kinase. *J. Immunol.* **1997**, *159*, 5206−10.

(6) (a) Majolini, M. B.; D'Elios, M. M.; Galieni, P.; Boncriastiano, M.; Lauria, F.; Del Prete, G.; Telford, J. L.; Baldari, C. T. Expression of the T-cell specific tyrosine kinase Lck in normal B-1 cells and in chronic lymphocytic leukemia B cells. *Blood* **1998**, *91*, 3390−96. (b) Von Knethen, A.; Abts, H.; Kube, D.; Diehl, V.; Tesch, H. Expression of p56lck in B-cell neoplasias. *Leuk. Lymphoma* **1997**, *26*, 551−62.

(7) (a) McCracken, S.; Kim, C. S.; Xu, Y.; Minden, M.; Miyamoto, N. G. An alternative pathway for expression of p56lck from type 1 promoter transcripts in colon carcinoma. *Oncogene* **1997**, *15*, 2929−37. (b) Nakamura, K.; Chijiiwa, Y.; Nawata, H. *Eur. J. Cancer* **1996**, *32A*, 1401−07. (c) Veillette, A.; Foss, F. M.; Sausville, E. A.; Bolen, J. B.; Rosen, N. Expression of the lck tyrosine kinase gene in human colon carcinoma and other non-lymphoid human tumor cell lines. *Oncogene Res.* **1987**, *1*, 357−74.

(8) Krystal, G. W.; DeBerry, C. S.; Linnekin, D.; Litz, J. Lck associates with and is activated by Kit in a small cell lung cancer line: inhibition of SCF-mediated growth by the Src family kinase inhibitor PP1. *Cancer Res.* **1998**, *58*, 4660−66.

(9) Frame, M. C. Src in cancer deregulation and consequences for cell behaviour. *Biochim. Biophys. Acta* **2002**, *1602*, 114−130.

(10) Haskell, M. D.; Slack, J. K.; Parsons, J. T.; Parsons, S. J. c-Src tyrosine phosphorylation of epidermal growth factor receptor, p190 RhoGAP, and focal adhesion kinase regulates diverse cellular processes. *Chem. Rev.* **2001**, *101*, 2425−40.

(11) Padmanabha, R.; Shu, Y.-Z.; Cook, L. S.; Veitch, J. A.; Donovan, M.; Lowe, S.; Huang, S.; Pirnik, D.; Manly, S. P. 1-Methoxy-agroclavine from penicillium SP. WC75209, a novel inhibitor of the Lck tyrosine kinase. *Bioorg. Med. Chem. Lett.* **1998**, *8*, 569−74.

(12) For a preliminary discussion on thiazole analogs, see: (a) Wityak, J.; Das, J.; Moquin, R. V.; Shen, Z.; Lin, J.; Chen, P.; Doweyko, A. M.; Pitt, S.; Pang, S.; Shen, D. R.; Fang, Q.; de Fex, H. F.; Schieven, G. L.; Kanner, S. B.; Barrish, J. C. Discovery and initial SAR of 2-amino-5-carboxamidothiazoles as inhibitors of the Src-family kinsae $p56^{lck}$. *Bioorg. Med. Chem. Lett.* **2003**, *13*, 4007−10. (b) Chen, P.; Norris, D.; Das, J.; Spergel, S. H.; Wityak, J.; Leith, L.; Zhao, R.; Chen, B-C.; Pitt, S.; Pang, S.; Shen, D. R.; Zhang, R.; deFex, H. R.; Doweyko, A. M.; McIntyre, K. W.; Shuster, D. J.; Behnia, K.; Schieven, G.; Barrish, J. Discovery of novel 2-(aminoheteroaryl)-thiazole-5-carboxamides as potent and orally active Src-family kinase $p56^{lck}$ inhibitors. *Bioorg. Med. Chem. Lett.* **2004**, *143*, 6061−66. (c) Lombardo, L. J.; Lee, F. Y.; Chen, P.; Norris, D.; Barrish, J. C.; Behnia, K.; Castaneda, S.; Cornelius, L.; Das, J.; Doweyko, A. M.; Fairchild, C.; Hunt, J. T.; Inigo, I.; Kamath, A.; Kan, D.; Marathe, P.; Pang, S.; Pitt, S.; Schieven, G. L.; Schmidt, R. J.; Tokarski, J.; Wen, M-L.; Wityak, J.; Borzilleri, R. M. Discovery of *N*-(2-chloro-6-methylphenyl)-2-(6-(4-(2-hydroxyethyl)piperazin-1-yl)-2-methylpyrimidin-4-ylamino)thiazole-5-carboxamide (BMS-354825), a dual Src/Abl kinase inhibitor with potent anti-tumor activity in preclinical assays. *J. Med. Chem.* **2004**, *47*, 6658−61. (d) Shah, N. P.; Tran, C.; Lee, F. Y.; Chen, P.; Norris, D.; Sawyers, C. L. Overriding imatinib resistance with a novel Abl kinase inhibitor. *Science* **2005**, *305*, 399−401. (e) Das, J.; Padmanabha, R.; Chen, P.; Norris, D. J.; Doweyko, A. M. P.; Barrish, J. C.; Wityak, J. Cyclic protein tyrosine kinase inhibitors. US 6596746 B2, 2003.

(13) For a description of assays, see: (a) Das, J.; Lin, J.; Moquin, R. V.; Shen, Z.; Spergel, S. H.; Wityak, J.; Doweyko, A. M.; deFex, H. R.; Fang, Q.; Pang, S.; Pitt, S.; Shen, D. R.; Schieven, G. L.; Barrish, J. C. Molecular design, synthesis and structure activity relationships leading to the potent and selective $p56^{lck}$ inhibitor BMS-243117. *Bioorg. Med. Chem. Lett.* **2003**, *13*, 2145−49. (b) Das, J.; Moquin, R. V.; Lin, J.; Liu, C.; Doweyko, A. M.; deFex, H. R.; Fang, Q.; Pang, S.; Pitt, S.; Shen, D. R.; Schieven, G. L.; Barrish, J. C.; Wityak, J. Discovery of 2-Amino-heteroaryl-benzothiazole-6-anilides as potent $p56^{lck}$ inhibitors. *Bioorg. Med. Chem. Lett.* **2003**, *13*, 2587−90.

(14) (a) Chen, P.; Norris, D.; Iwanowicz, E. J.; Spergel, S. H.; Lin, J.; Gu, H. H.; Shen, Z.; Wityak, J.; Lin, T-A.; Pang, S.; deFex, H. F.; Pitt, S.; Shen, D. R.; Doweyko, A. M.; Bassolino, D. A.; Roberge, J. Y.; Poss, M. A.; Chen, B-C.; Schieven, G. L.; Barrish, J. C. Discovery and initial SAR of imidazoquinoxalines as inhibitors of Src-family kinase $p56^{lck}$. *Bioorg. Med. Chem. Lett.* **2002**, *12*, 1361−64. (b) Snow, R. J.; Cardozo, M. G.; Morwick, T. M.; Busacca, C. A.; Dong, Y.; Eckner, R. J.; Jacober, S.; Jakes, S.; Kapadia, S.; Lukas, S.; Panzenbeck, M.; Peet, G. W.; Peterson, J. D.; Prokopowicz, A. S., III; Sellati, R.; Tolbert, R. M.; Tschantz, M. A.; Moss, N. Discovery of 2-phenylamino-imidazo[4,5-h]isoquinolin-9-ones: A new class of inhibitors of Lck kinase. *J. Med. Chem.* **2002**, *45*, 3394−3405.

(15) Yamaguchi, H.; Hendrickson, W. A. Structural basis for activation of human lymphocyte kinase Lck upon tyrosine phosphorylation. *Nature* **1996**, *384*, 484−89.

(16) Zhu, X.; Kim, J. L.; Rose, P. E.; Stover, D. R.; Toledo, L. M.; Zhao, H.; Morgenstern, K. A. Structural analysis of the lymphocyte-specific kinase Lck in complex with non-selective and Src family selective kinase inhibitors. *Structure* **1999**, *7*, 651−61.

(17) Sicheri, F.; Kuriyan, J. Structures of Src-family tyrosine kinases. *Curr. Opin. Struct. Biol.* **1997**, *7*, 777−85.

(18) Sicheri, F.; Moarefi, I.; Kuriyan, J. Crystal structure of the Src-family tyrosine kinase Hck. *Nature* **1997**, *385*, 602−9.

(19) Chen, P.; Doweyko, A. M.; Norris, D.; Gu, H. H.; Spergel, S. H.; Das, J.; Moquin, R. V.; Lin, J.; Wityak, J.; Iwanowicz, E. J.; McIntyre, K. W.; Shuster, D. J.; Behnia, K.; Chong, S.; deFex, H.; Pang, S.; Pitt, S.; Shen, D. R.; Thrall, S.; Stanley, P.; Kocy, O. R.; Witmer, M. R.; Kanner, S. B.; Schieven, G. L.; Barrish, J. C. Imidazoquinoxaline Src-family kinase p56Lck inhibitors: SAR, QSAR, and the discovery of (*S*)-*N*-(2-chloro-6-methylphenyl)-2-(3-methyl-1-piperazinyl)imidazo[1,5-a]pyrido[3,2-e]pyrazin-6-amine (BMS-279700) as a potent and orally active inhibitor with excellent in vivo anti-inflammatory activity. *J. Med. Chem.* **2004**, *47*, 4517−29.

(20) (a) Tokarski, J. S.; Newitt, J. A.; Chang, C. Y. J.; Cheng, J. D.; Wittekind, M.; Kiefer, S. E.; Kish, K.; Lee, F. Y. F.; Borzilleri, R.; Lombardo, L. J.; Xie, D.; Zhang, Y.; Klei, H. E. The structure of dasatinib (BMS-354825) bound to activated Abl kinase domain elucidates its inhibitory activity against imatinib-resistant Abl mutants. *Cancer Res.* **2006**, *66*, 5790−97. (b) Nagar, B.; Bornmann, W. G.; Pellicena, P.; Schindler, T.; Veach, D. R.; Miller, W. T.; Clarkson, B.; Kuriyan, J. Crystal structures of the kinase domain of c-Abl in complex with the small molecule inhibitors PD173955 and imatinib (STI-571). *Cancer Res.* **2002**, *62*, 4236−43. (c) Schindler, T.; Bornmann, W.; Pellicena, P.; Miller, W. T.; Clarkson, B.; Kuriyan, J. Structural mechanism for STI-571 inhibition of Ableson Tyrosine Kinase. *Science* **2000**, *289*, 1938−42.

(21) (a) Newton, R. C.; Decicco, C. P. Therapeutical potential and strategies for inhibiting tumor necrosis factor-α. *J. Med. Chem.* **1999**, *42*, 2295−2314. (b) Feldmann, M.; Brennan, F. M.; Maini, R. N. Role of cytokines in rheumatoid arthritis. *Annu. Rev. Immunol.* **1996**, *14*, 397−440.

(22) (a) Jarvis, B.; Faulds, D. Etanercept: a review of its use in rheumatoid arthritis. *Drugs* **1999**, *57*, 945−966. (b) Lipsky, P. E.; van der Heijde, D. M. F. M. E.; St. Clair, W.; Furst, D. E.; Breedveld, F. C.; Kalden, J. R.; Smolen, J. S.; Weisman, M.; Emery, P.; Feldmann, M.; Harriman, G. R.; Maini, R. N. Infliximab and methotrexate in the treatment of rheumatoid arthritis. *N. Engl. J. Med.* **2000**, *343*, 1594−1602. (c) Rutgeerts, P. J. Efficacy of infliximab in Crohn's disease—induction and maintenance of remission. *Aliment. Pharmacol. Ther.* **1999**, *13* (Suppl 4), 9−15.

(23) (a) Falta, M. T.; Kotzin, B. L. In *T Cells In Arthritis*; Miossec, P., van den Berg, W. B., Firestein, G. S., Eds.; Birkhauser verlag: Basel, Switzerland, 1998; pp 202−31. (b) Korganow, A-S.; Ji, H.; Mangialaio, S.; Duchatelle, V.; Pelanda, R.; Martin, T.; Degott, C.; Kikutani, H.; Rajewsky, K.; Pasquali, J.-L.; Benoist, C.; Mathis, D. From systemic T cell self-reactivity to organ-specific autiimmune disease via immunoglobulins. *Immunity* **1999**, *10*, 451−61.

(24) Kremer, J. M.; Westhovens, R.; Leon, M.; Di Giorgio, E.; Alten, R.; Steinfeld, S.; Russell, A.; Dougados, M.; Emery, P.; Nuamah, I. F.; Williams, G. R.; Becker, J.-C.; Hagerty, D. T.; Moreland, L. W. Treatment of rheumatoid arthritis by selective inhibition of T-cell activation with fusion protein CTLA4Ig. *N. Engl. J. Med.* **2003**, *349*, 1907−15.

(25) Talpaz, M.; Shah, N. P.; Kantarjian, H.; Donato, N.; Nicoll, J.; Paquette, R.; Cortes, J.; O'Brien, S.; Nicaise, C.; Bleickardt, E.; Blackwood-Chirchir, M. A.; Iyer, V.; Chen, T-T.; Huang, F.; Decillis, A. P.; Sawyers, C. L. Dasatinib in imatinib-resistant Philadelphia chrosome-positive leukemias. *N. Engl. J. Med.* **2006**, *354*, 2531−41.

JM060727J